Redox Biology 63 (2023) 102745

Contents lists available at ScienceDirect

Redox Biology

journal homepage: www.elsevier.com/locate/redox

β-Nicotinamide mononucleotide activates NAD+/SIRT1 pathway and attenuates inflammatory and oxidative responses in the hippocampus regions of septic mice

Hui-ru Li [a,b,1], Qiang Liu [b,c,1], Cheng-long Zhu [b,1], Xiao-yang Sun [a,b], Chen-yan Sun [b], Chang-meng Yu [b,c], Peng Li [b], Xiao-ming Deng [a,b,c,**], Jia-feng Wang [b,*]

[a] School of Anesthesiology, Weifang Medical University, Weifang, 261053, China
[b] Faculty of Anesthesiology, Changhai Hospital, Naval Medical University, Shanghai, China
[c] Jiangsu Province Key Laboratory of Anesthesiology, Xuzhou Medical University, Xuzhou, Jiangsu, China

ARTICLE INFO

Keywords:
Sepsis-associated encephalopathy
β-Nicotinamide mononucleotide
Nicotinamide adenine dinucleotide
Sirtuin 1
Inflammation
Oxidative stress

ABSTRACT

Sepsis-associated encephalopathy (SAE) is one of the common serious complications in sepsis, and the pathogenesis of SAE remains unclear. Sirtuin 1 (SIRT1) has been reported to be downregulated in the hippocampus and SIRT1 agonists can attenuated the cognitive dysfunction in septic mice. Nicotinamide adenine dinucleotide (NAD+) is a key substrate to maintain the deacetylation activity of SIRT1. As an intermediate of NAD+, β-Nicotinamide Mononucleotide (NMN) has been reported to be promising in treating neurodegenerative diseases and cerebral ischemic injury. Thus we sought to investigate the potential role of NMN in SAE treatment. The SAE model was established by cecal ligation and puncture (CLP) *in vivo*, and neuroinflammation model was established with LPS-treated BV-2 cells *in vitro*. Memory impairment was assessed by Morris water maze and fear conditioning tests. As a result, the levels of NAD+, SIRT1 and PGC-1α were significantly reduced in the hippocampus of septic mice, while the acetylation of total lysine, phosphorylation of P38 and P65 were enhanced. All these changes induced by sepsis were inverted by NMN. Treating with NMN resulted in improved behavior performance in the fear conditioning tests and Morris water maze. Apoptosis, inflammatory and oxidative responses in the hippocampus of septic mice were attenuated significantly after NMN administration. These protective effect of NMN against memory dysfunction, inflammatory and oxidative injuries were reversed by the SIRT1 inhibitor, EX-527. Similarly, LPS-induced activation of BV-2 cells were attenuated by NMN, EX-527 or SIRT1 knockdown could reverse such effect of NMN *in vitro*. In conclusion, NMN is protective against sepsis-induced memory dysfunction, and the inflammatory and oxidative injuries in the hippocampus region of septic mice. The NAD+/SIRT1 pathway might be involved in one of the mechanisms of the protective effect.

1. Introduction

Sepsis is a life-threatening organ dysfunction caused by dysregulated host responses to infectious factors, and remains to be a major cause of death worldwide [1,2]. Sepsis-associated encephalopathy (SAE) is a common complication of sepsis characterized by diffuse brain dysfunction secondary to infection with the absence of overt central nervous system (CNS) infection, with a prevalence of up to 70% of septic patients, especially in the elderly, neonates and patients with chronic diseases [3]. The pathophysiology is complex and microglial activation in the hippocampus may be a key process in the development of SAE [4]. Early control of the underlying infection, and the correction of organ dysfunction and metabolic alterations (hypoglycemia, hyperglycemia, hypercapnia, hypernatremia) are essential for SAE, but unfortunately, there is no effective medication targeting at SAE in clinical settings [5].

Nicotinamide adenine dinucleotide (NAD+) plays a vital role in energy metabolism, immunoinflammatory and oxidative stress response in all living cells as an important co-enzyme and substrate, such as

* Corresponding author. Faculty of Anesthesiology, Changhai Hospital, Naval Medical University, 168 Changhai Road, Shanghai, 200433, China.
** Corresponding author. Faculty of Anesthesiology, Changhai Hospital, Naval Medical University, 168 Changhai Road, Shanghai, 200433, China.
E-mail addresses: dengphd@smmu.edu.cn (X.-m. Deng), jfwang@smmu.edu.cn (J.-f. Wang).
[1] These authors contributed equally to this work.

https://doi.org/10.1016/j.redox.2023.102745
Received 17 December 2022; Received in revised form 28 April 2023; Accepted 12 May 2023
Available online 13 May 2023

sirtuins, poly (ADP-ribose) polymerase 1(PARP1), and cluster of differentiation 38 (CD38) [6,7]. Growing evidence has indicated that NAD + depletion happens in the elderly and in patients with neurodegenerative diseases. Physiological and pharmacological interventions to maintain cellular NAD + levels may delay aging and prevent some age-related diseases [8,9]. Sirtuins (SIRTs) are evolutionally-conserved family of regulatory proteins that function as NAD + -dependent class III histone deacetylases (HDACs), which is composed of seven histone deacetylases and ADP-ribosyltransferase proteins (SIRT1-7) in mammals [10]. As the most widely investigated member of the SIRT family, SIRT1 regulates cell biology and metabolism by deacetylating histones or other multiple cytoplasmic substrates and inhibiting proinflammatory kinases or regulating transcriptional factors, such as peroxisome proliferator-activated receptor-gamma co-activator 1α (PGC-1α), forkhead boxO3a (FoxO3a), nuclear factor kappa B p65 (NF-κB p65), p38 mitogen-activated protein kinase (p38 MAPK), and p300 [11–15]. A large amount of evidence has confirmed that SIRT1 plays an important role in the regulation of oxidative stress, inflammation, mitochondrial function, autophagy, apoptosis, neuroprotection and aging-related diseases [16–19]. In addition, SIRT1 could attenuate sepsis-induced organ damage [20]. Conventionally, SIRT1 function is highly dependent on NAD+ in mammalian cells, SIRT1 is a highly conserved NAD + -dependent deacetylase, and its deacetylation reaction requires NAD as a cosubstrate. High levels of NAD + can activate SIRT1 [21]. And most NAD+ is recycled via salvage pathways, in which nicotinamide (NAM) is recycled and transformed into nicotinamide mononucleotide (NMN), via nicotinamide phosphoribosyl transferase (NAMPT). Then NMN is converted into NAD + by nicotinamide mononucleotide adenylyl transferases (NMNATs). A growing body of evidences show that the metabolite NAD+ is a mediator of both antiviral and anti-inflammatory mechanisms. Interestingly, NAD+ is decreased during sepsis [22,23], and NAD + could improve cellular energy supply and inhibit cell apoptosis and dysfunction in immune cells and endothelial cells, suggesting that elevated NAD + levels could potentially ameliorate the evolution of sepsis [24].

NMN is a biologically active nucleotide that could be synthesized endogenously. In general, NMN is naturally present as two irregular forms, α and β, and the β anomer is the active form of NMN. As a precursor of NAD+, NMN is a pivotal intermediate in NAD + biosynthesis and has been considered as a promising anti-aging health care product [25,26]. It was reported that exogenous NMN supplementation could reduce oxidative stress response and promote vascular endothelial formation by restoring NAD + levels [27,28]. In addition, NMN significantly attenuated the excessive inflammatory cell infiltration and microvascular embolization in the murine lungs infected by SARS-CoV-2, and improved the survival rate of infected mice [29]. It had been observed that the administration of β-NMN could modulate the macrophage phenotype and thereby ameliorated the dysregulated inflammatory response during sepsis [30]. However, to our knowledge, it was unclear whether NMN was protective against SAE.

Thus, the main purpose of our study was to explore the therapeutic effect of NMN in SAE mice, and the role of NAD+/SIRT1 pathway in the underlying mechanism of neuroprotective effect of NMN.

2. Materials and methods

2.1. Animals and ethics statement

Adult, male, 8-10-week-old C57BL/6J mice were purchased from GemPharmatech Laboratory Animals (Nanjing, China) and maintained in our animal house for at least 2 weeks prior to the experiment. All animals were maintained in specific pathogen-free conditions under a temperature of 21 °C–23 °C, relative 40%–60% humidity, and subjected to a 12 h light/dark cycle with unlimited access to standard chow diet and water. The experimental protocol for animal study was approved by the Animal Research Ethics Committee of Changhai Hospital and complied with relevant regulations.

2.2. Establishment of CLP model and drug administration

Septic mice were induced by cecal ligation and puncture (CLP) as described in our previous studies [31]. In general, mice were anesthetized with 2–3% sevoflurane. After barbering and disinfection, a midline abdominal incision was made to explore and expose the cecum. Before ligation and puncture, the cecal contents were gently pushed toward the distal cecum. Half of the cecal root was ligated, and the cecum was penetrated with a 22G needle through and through, with some feces extruded. Finally, the cecum was returned into the peritoneal cavity and the skin was sutured layer by layer. In sham-operated mice, the cecum was exposed without ligation or puncture. Tramadol (20 mg/kg body weight) was subcutaneously injected for postoperative analgesia and all mice were resuscitated by injecting 1 ml normal saline subcutaneously. Mice will be deeply anesthetized 24 h after surgery, and the whole blood was obtained by heart puncture, then mice will be quickly sacrificed, and the hearts of mice were perfused with continuous phosphate buffered saline (PBS) until the liquid from auricula dextra became clear. Hippocampal tissues were harvested for subsequent relevant detection, or the whole brain tissues of mice were fixed with 4% paraformaldehyde.

β-Nicotinamide Mononucleotide (C11H15N2O8P, CAS, 1094-61-7, purity ≥99% by HPLC) was purchased from Zheyan Biotechnology (Shanghai, China). NMN was dissolved in sterile PBS and injected intraperitoneally (500 mg/kg) in mice immediately after surgery. Selisistat (EX-527), a selective SIRT1 inhibitor, was purchased from Selleck (Cat: S1541, USA), dissolved in Dimethyl Sulfoxide (DMSO, Sigma, USA), and injected intraperitoneally (5 mg/kg) immediately after surgery. The dose of NMN and EX-527 were referred to previous studies [32,33].

2.3. BV-2 cell culture and drug treatment

Mouse microglia cell line BV-2 was obtained from Tongpai Biological Technology (Shanghai, China), and used to investigate microglia *in vitro*. The cells were cultured in dulbecco's modified eagle medium (DMEM) high glucose medium (Gibco, Langley, USA) supplemented with 10% fetal bovine serum (FBS, Sigma-Aldrich, St. Louis, USA), 1% penicillin and streptomycin (Gibco, Langley, USA) at 37 °C in a 5% CO2 sterile incubator. BV-2 cells were pretreated with EX-527 (10 μM) for 1 h, and then stimulated with 1 μg/ml lipopolysaccharide (LPS, Sigma Corporation, USA) and/or NMN (1 mM) for 24 h to establish the inflammatory model *in vitro* [34]. The dose of NMN and EX-527 were referred to previous studies [35–37]. All reagents and procedures were strictly sterile, and all operations were completed in a biological safety cabin.

2.4. Morris water maze test

A standard 5-day water maze test was performed to measure learning and memory abilities [38,39]. The concrete protocol was described as follows: The apparatus was composed of a circular water pool with a diameter of 120 cm and a height of 30 cm, containing an escape platform with a diameter of 6 cm inside. The pool was divided into four quadrants with equal area and the platform was 1 cm below the water surface located in the center of target quadrant. Appropriate amounts of titanium dioxide were added to the water pool so that the mice could not see the platform in the blurred water with a temperature of 23 ± 1 °C and curtains were covered around the pool in order to prevent the surrounding environment from interfering with the experiment. Each mouse in all groups was trained to find the platform for four consecutive days. On the same day, each mouse was placed into the water from four different quadrants facing the pool wall independently. After the end of trial in one quadrant, the mouse was dried with a towel and kept warm in a cage. The time for mice to reach the platform was recorded

separately after entering the water in each quadrant as the latency period. If the mouse could not reach the escape platform within 60 s, it was manually guided to the platform and allowed to stay on the platform for 10 s with the escape latency was recorded as 60 s. The latency of the four quadrants was averaged to calculated for each mouse on the same day. On day 5, the platform within the target quadrant was removed for probe test. Mice were placed in water from the contralateral region of the target quadrant, and the number of times they crossed the original platform area in 60 s as well as the time spent in the target quadrant were recorded. The video tracking and the time were recorded automatically via professional software (SuperMaze software, Shanghai Xinruan Information Technology Co.,Ltd).

2.5. Fear conditioning test (FC)

Fear conditioning device (XR-XZ301, Xinruan Information Technology, Shanghai, China) was used to test the capacity of conditioned memory. In brief, All the mice were placed into a chamber with stainless steel floor and trained to adapt to the training environment for 3 min, followed by 30 s of tone stimulation (65 dB, 3 kHz), then electrical stimulation (0.75 mA) to foot was performed at the end of the last 3 s of the sound, tonal and electrical stimulation was reemerged after 30 s at a total of 3 times. After 24 h, the mice were placed in the training environment without any stimulation for 3 min. After 2 h, the animals were placed in the training room again and subjected to tone stimulation for 3 min without foot shock. The freezing time of the environmental and tone stimulation were recorded during the 3-min period. Freezing behavior is defined as the absence of visible movement other than breathing.

2.6. Immunofluorescence

The brain tissues of mice were obtained 24 h after surgery, and paraffin sections (4-μm thick) were made. The sections were blocked with 10% donkey serum for 60min, and incubated with the primary antibody (anti-IBA-1, 1:200, Abcam, USA; anti-CD68, 1:200, Abcam; anti-SIRT1, 1:200, Proteintech, China) at 4 °C overnight. After washing, the secondary antibody (1:1000) was incubated at room temperature for 1.5 h in the dark. Nuclear staining was performed with 4′, 6-diaminidine-2-phenylindole (DAPI). After sealed, the slices were photographed and analyzed under a fluorescence microscope (Nikon, Japan). For quantitative analysis of immunofluorescence results of microglia cells, we referred to the previous study [40]. Three independent microscopic fields in the DG area were randomly selected, and three sections in each group were analyzed. Fluorescence microscopy (Nikon, Japan) was performed to visualize Iba-1-positive cells (green-stained cells) and CD68-positive cells or SIRT1-positive cells (red-stained cells). Cell counts and CD68/Iba-1 co-localization or SIRT1/Iba-1 co-localization analyses were carried using the ImageJ software. DAPI emits blue light at an ultraviolet excitation wavelength of 377 nm and an emission wavelength of 447 nm; SpGreen has an excitation wavelength of 494 nm and an emission wavelength of 527 nm. SpRed has an excitation wavelength of 586 nm and an emission wavelength of 628 nm.

2.7. Terminal Deoxynucleotidyl Transferase-mediated dUTP Nick End Labeling (TUNEL) staining of brain tissues

Brain tissues were harvested 24 h after the operation and made into paraffin sections (3-μm thick). Then the sections were deparaffinized, rehydrated, treated with proteinase K, and permeabilized with 0.1% Triton at room temperature for 20 min. After equilibrium at room temperature, reaction solution (TDT enzyme, dUTP and buffer at 1:5:50 ratio) was added and incubated at 37 °C for 2 h. Nuclei were counterstained with DAPI, and the slices were sealed. Fluorescence microscopy (Nikon, Japan) was performed to visualize TUNEL-positive cells (green-stained cells). The apoptosis rate was expressed as the average of the percentage of TUNEL-positive staining area in the total image area of the whole microscopic field in each of the three fields in the DG region, and 6 sections in each group were analyzed. Tunel assay kit (Servicebio, G1501) is labelled with FITC, DAPI emits blue light at an ultraviolet excitation wavelength of 377 nm and an emission wavelength of 447 nm; FITC has an excitation wavelength of 494 nm and an emission wavelength of 527 nm, and emits green.

2.8. Determination of NAD + concentration

According to the previous studies [41,42], NAD + contents in fresh hippocampus obtained 24 h after surgery and BV-2 cells stimulated with LPS for 24 h were measured via using (NAD+)/(NADH) assay kit (WST-8 method, Beyotime, cat: S0175, Shanghai, China). More particularly, for the preparation of cell samples, 1×10^6 BV-2 cells were collected and lysed with 200 μl NAD+/NADH extract buffer after the culture medium was removed. Subsequently, they were centrifuged at 12,000 g for 10 min at 4 °C, and the supernatant was used as the sample to be tested. For the preparation of tissue samples, after washing the tissue with pre-cooled PBS, the hippocampus was weighed and homogenized with 400 μl NAD+/NADH extract buffer. Similar to cell samples, the supernatant was used as the sample to be tested for later use after centrifugation. After reagent preparation, firstly, the total amount of NAD+ and NADH in the sample was determined: 20 μl the tested sample was absorbed into a 96-well plate, and 90 μl alcohol dehydrogenase working solution was added to the sample, incubated at 37 °C for 10 min, NAD+ in the sample was converted to NADH. Then 10 μl of the chromogenic agent was added to each well, incubated at 37 °C for 30 min in the dark. At this time, orange formazan was formed. The total amount of NAD + plus NADH was obtained by measuring the absorbance at 450 nm. Then, the content of NADH was determined as follows. 50–100 μl sample was transferred into a centrifuge tube and heated at 60 °C for 30 min to decompose NAD+. Subsequently, 90 μl working solution with alcohol dehydrogenase was added to the 96-well plate. Then, 10 μl chromogenic agent was added to each well, mixed appropriately, incubated at 37 °C in the dark for 30 min, and the absorbance at 450 nm was measured to obtain the amount of NADH. The difference between the amount of NADH and the total amount of NADH plus NAD+ was calculated as the amount of NAD+.

2.9. Enzyme-linked immunosorbent assay (ELISA)

The concentration of inflammatory mediators (IL-6, IL-1β and TNF-α) in hippocampal homogenate and serum obtained 24 h after surgery, or supernatant of cell culture medium collected after stimulating with LPS for 24 h was measured by enzyme-linked immunosorbent assay according to the manufacturer's instructions (Invitrogen, cat: 88-7324-88, 88-7064-88, 88-7013-88, USA). The results were read at 450 nm with a spectrophotometer (Synergy2, BioTek, USA). Hippocampal protein concentrations were quantified using a BCA quantification kit (Thermo, cat: 23228, 23224, Rockford, IL, USA).

2.10. Measurement of ROS production

DHE probe (Sigma-Aldrich, D7008, USA) was used to measure the ROS production in the hippocampus of mice *in vivo*. Firstly, brain tissues of mice were obtained 24 h after the operation and made into frozen sections (8-μm thick), then we used DHE stain (10 μM) to treat the frozen slices and incubated these slices at 37 °C for about 30 min in a dark environment. Next, we applied DAPI to counterstain the cell nucleus of brain tissues for 5 min. Following this, these slices were washed with water and the images in the DG area were captured under fluorescence microscope (Nikon, Japan) with an excitation (Ex) wavelength at 525 nm and an emission (Em) wavelength at 610 nm. Relative quantification of fluorescence intensity was performed by ImageJ software. DCFH-DA probe (Beyotime, cat: S0033S, Shanghai, China) was used to measure the intracellular ROS levels *in vitro*. After 24 h of treatment, the medium

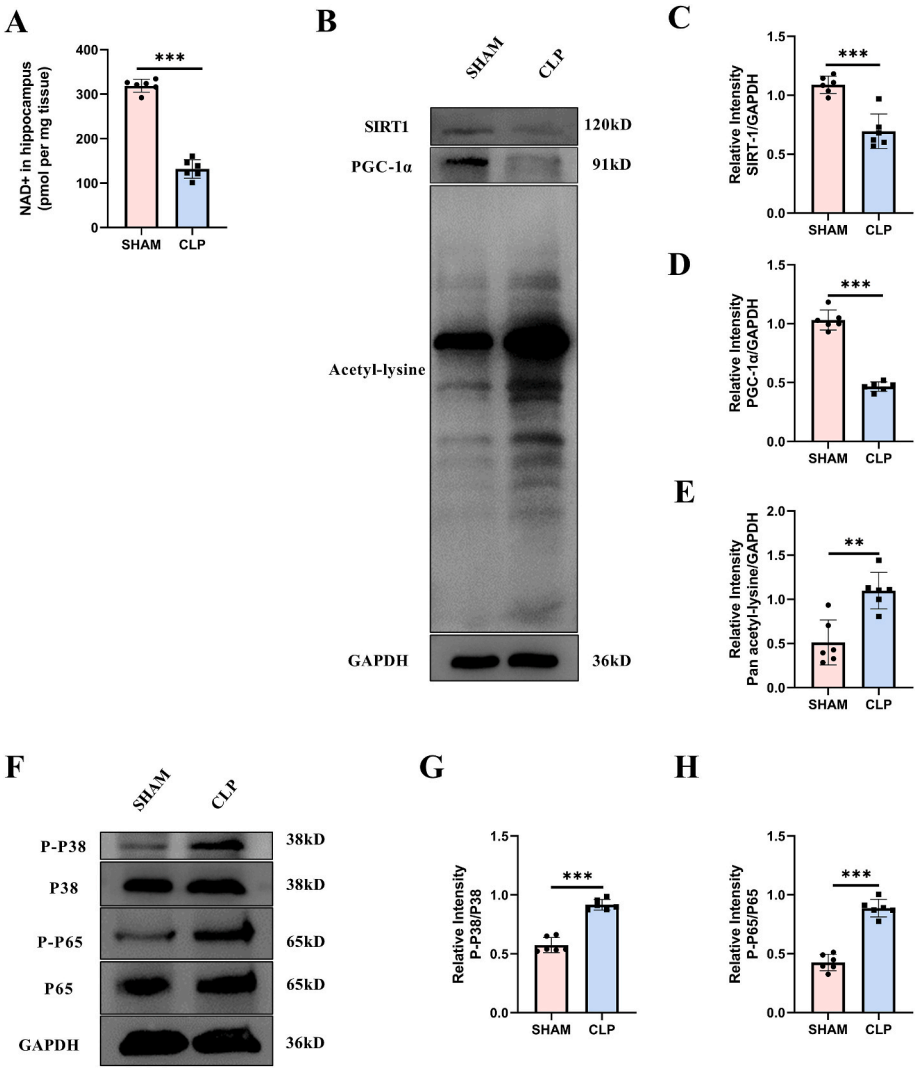

Fig. 1. NAD+/SIRT1 pathway was inhibited while p38 MAPK and NF-κB were actiavted in the hippocampus region of CLP mice at 24 h after surgery. **(A)** NAD + content. **(B–E)** Expression and relative quantification of SIRT1 and PGC-1α, and the level of lysine acetylation. **(F–H)** Phosphorylation and relative quantification of P38 and P65. Unpaired Student's-*t* test was used. The values were presented as mean ± SD (**p < 0.01, ***p < 0.001, n = 6 for each group).

supernatant in the 6-well plate was removed, and the living BV-2 cells were washed with pre-warmed PBS and stained with 1 mL DCFH-DA (10 μM) staining solution. The stained cells were incubated in a cell incubator at 37 °C for 20 min in the dark. The dye solution was discarded, and the cells were washed three times with serum-free culture medium. At last, the cells were collected and the intensity of fluorescence was detected by flow cytometry operated on FACSCanto II flow cytometer (BD Bioscience, San Jose, CA, USA) at the excitation wavelength of 488 nm and the emission wavelength of 525 nm. And the data were analyzed using FlowJo V7.6 (Tree Star, Ashland, OR, USA).

2.11. Assessment of superoxide dismutase (SOD) and malondialdehyde (MDA)

According to the instructions, the content of MDA and SOD activity in the hippocampus tissues obtained 24 h after surgery were measured by using the correlated detection kits from Nanjing Jiancheng Institute of Biological Engineering, cat: A003-1, A001-1, Jiangsu, China, and those in BV-2 cells collected after stimulating with LPS for 24 h were detected by the kits from Beyotime, cat: S0131S, S0101S, Shanghai, China.

2.12. Western blot detection

The total proteins were extracted from mice hippocampal tissues obtained 24 h after surgery or BV-2 cells collected after stimulating with LPS for 24 h with RIPA lysis buffer (Beyotime, cat: P10013B, Shanghai, China) supplemented with protease and phosphatase inhibitors. Subsequently, the protein concentrations were quantified by using the BCA Protein Quantification Assay Kit (ThermoScience, cat: 23228, 23224, Rockford, IL, USA). Appropriate protein samples were separated by 10% sodium dodecyl sulfate and polyacrylamide gel electrophoresis (SDS-PAGE) and then transferred to polyvinylidene fluoride (PVDF) membranes. The membranes were blocked with 5% skim milk for 1 h, and incubated with specific primary antibodies overnight at 4 °C. After washed with TBST buffer for 3 times, the strips were incubated with goat anti-mouse IgG-HRP and goat anti-rabbit IgG-HRP (1:2000, Engibody Biotechnology, Milwaukee, WI, USA) for 2 h at the room temperature. After washed with TBST buffer again, the blots were imaged by electrochemiluminescence (ECL) detection kit (ThermoScientifc, cat: WP20005, Rockford, USA) and Imaging System (Bio-Rad, USA). The primary antibodies included SIRT1(1:1000, CST, Boston, USA), PGC-1α (1:1000, Abclonal, Wuhan, China), acetyl-Lysine (1:1000, CST, Boston, USA), P-p38 (1:1000, CST, Boston, USA), P38 (1:1000, CST, Boston, USA), P-p65 (1: 1000, CST, Boston, USA), P65 (1:1000, CST, Boston,

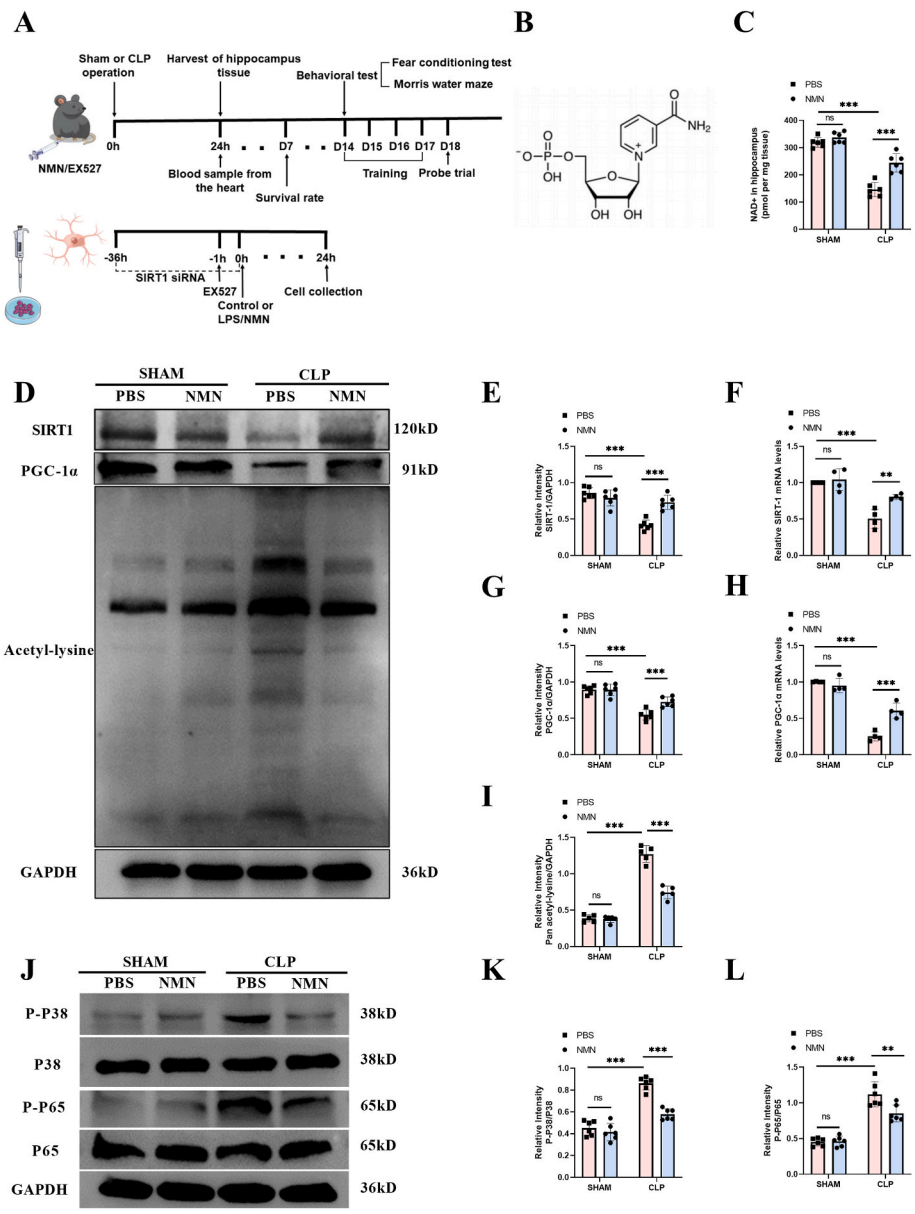

Fig. 2. NMN attenuated sepsis-induced changes of the levels of NAD+, SIRT1, PGC-1α, and lysine acetylation of proteins and inhibited the phosphorylation of P38 and P65 in hippocampus of septic mice at 24 h after surgery. (A) Schematic representation of timeline and experimental design. **(B)** Structural formula of β-Nicotinamide Mononucleotide (NMN). **(C)** NAD+ in hippocampus. **(D–I)** Expression and relative quantification of SIRT1 and PGC-1α, and level of lysine acetylation. **(J–L)** Phosphorylation and relative quantification of P38 and P65. Tukey post-hoc test following a two-way ANOVA was used. The values were presented as mean ± SD (**p < 0.01, ***p < 0.001, n = 4 to 6 for each group).

USA), GAPDH (1:2000, Engibody Biotechnology, Milwaukee, WI, USA).

2.13. Quantitative real-time PCR (RT-qPCR)

Total RNA was extracted using the RNeasy Plant Mini Kit (Qiagen, Germany, cat:74904) as directed by the manufacturer. The RNA concentration was detected by nanodrop and adjusted to the same level. mRNA was reverse transcribed using PrimeScript RT reagent Kit (TAKARA, cat: #RR036; Tokyo, Japan), and PCR was conducted using TB Green™ Premix Ex Taq™ (Tli RNaseH Plus) (TAKARA, cat: #RR420A; Tokyo, Japan) and StepOnePlus real-time PCR system (Applied Biosystems). Data were normalized to the expression of beta-2-microglobulin gene (B2M). The specific primer sequences of genes are displayed in Table S1 in the supplementary files.

2.14. Bisulfite sequencing PCR (BSP) detection

The genomic DNA was isolated from BV-2 cells using the TIAN amp genomic DNA kit (cat: DP304). The purified DNA was treated with bisulfite using the EZ DNA Methylation-Gold™ Kit (ZYMO, cat: D5005, USA) under the manual instruction. The promoter of SIRT1 sequence was amplified from the converted DNA by PCR, and the purified PCR products were cloned into pMD-19 T vector (Takara, China) for sequencing. We sequenced 10 individual clones. Primers were listed in Supplementary Table S1.

2.15. Quantifying the concentration of s-adenosyl methionine (SAM) in BV-2 cells

For the detection of SAM concentration, the procedure was performed according to the instructions of the commercial ELISA kit (Cloud-Clone Corp, cat: #CEG414Ge; Wuhan, China). Briefly, cells were resuspended in fresh lysis buffer, and centrifuged at 1500 g for 10 min at 4 °C to recover the supernatant for assay. 50 μl sample was added to the microplate coated with the specific antibody, followed by addition of detection solution A, incubation at 37 °C for 1 h. Then washing to remove the unbound substance and the detection solution B was added. After incubation at 37 °C for 30 min and thorough washing, the substrate TMB was added for color development, and the absorbance OD value at 450 nm wavelength was measured immediately after adding the

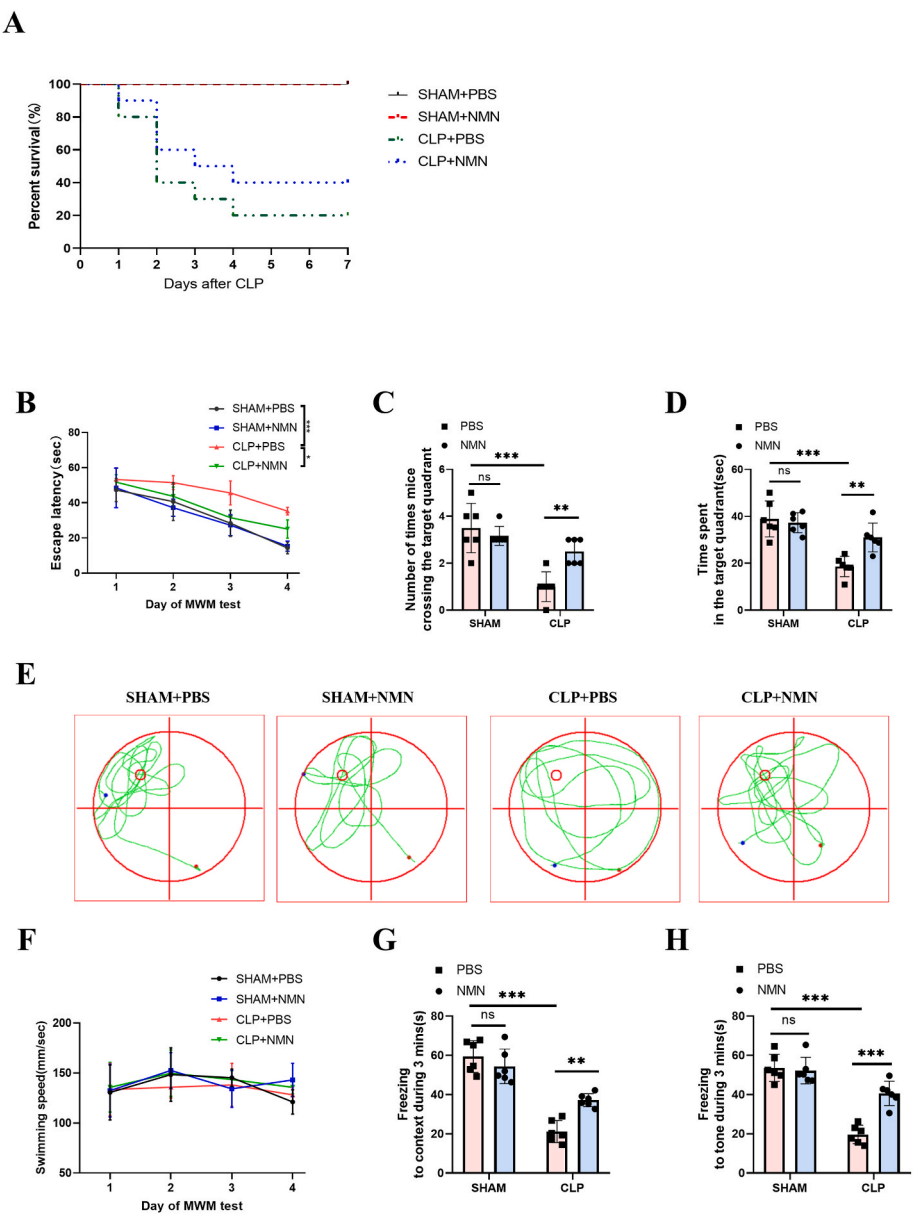

Fig. 3. NMN improved the impaired memory in CLP mice. **(A)** Seven-day survival rate of mice. **(B)** Escape latency time. **(C)** Number of crossings over the target quadrant in the Morris water maze beginning on day 18 after CLP. **(D)** Time spent in the target quadrant. **(E)** Representative swimming paths on the test day. The smaller red circle indicates the location of the training platform, which was removed during the test. **(F)** swimming speed in the Morris water maze. **(G)** The freezing time in response to the context in the fear conditioning test. **(H)** The freezing time in response to the tone in the fear conditioning test. Log-rank test was used in (A), Tukey post-hoc test following a two-way ANOVA was used was used in other figures. The values were presented as mean ± SD (*$p < 0.05$, **$p < 0.01$, ***$p < 0.001$, $n = 10$ in each group for survival rate; $n = 6$ in each group for Morris water maze and fear conditioning tests).

termination solution. The sample concentration was calculated according to corresponding OD value.

2.16. Small interfering RNA (siRNA) transfection

According to the manufacturer's instructions, BV-2 cells were transiently transfected with SIRT1 siRNA (sc-40987) or non-targeting siRNA (sc-37007) as a control siRNA (Santa Cruz Inc, CA, USA). Briefly, 2×10^5 BV-2 cells were seeded into 6 well plates till 60–80% confluent and transfected with SIRT1 siRNA or negative control siRNA for 36 h at 37 °C with Lipofectamine 3000 (Invitrogen, Carlsbad, CA, USA) according to the manufacturer's manual. Post-transfection, cells were used for subsequent functional experiments. The impact of knockout on SIRT1 was assessed by western blotting analysis.

2.17. Statistical analysis

GraphPad Prism 8.0 software was used for statistical analysis of all experimental data. Measurement data were described as mean and standard deviation (SD). Data were normally distributed as tested using the Shapiro-Wilk test. Unpaired Student's *t*-test was used to compare the two groups of data, and the comparisons between groups of three or more groups were performed using one-way ANOVA followed by Tukey post-hoc test. For comparisons involving two factors, such as CLP and NMN treatment or CLP and time points, two-way ANOVA followed by Tukey post-hoc test was used. The survival rate of animal experimental models was compared by log-rank test. $P < 0.05$ were considered statistically significant.

3. Results

3.1. NAD+/SIRT1 pathway was inhibited while inflammation was enhanced in the hippocampus of septic mice

In order to clarify the changes of NAD+/SIRT1 pathway in the hippocampus tissue of septic mice, we measured the levels of NAD+, SIRT1 and PGC-1α in the hippocampus. The results showed that CLP mice had significantly less NAD+ in the hippocampus than the sham-operated mice (Fig. 1A). Similarly, the expressions of SIRT1 and PGC-1α were significantly reduced in CLP mice, accompanied by the enhanced total

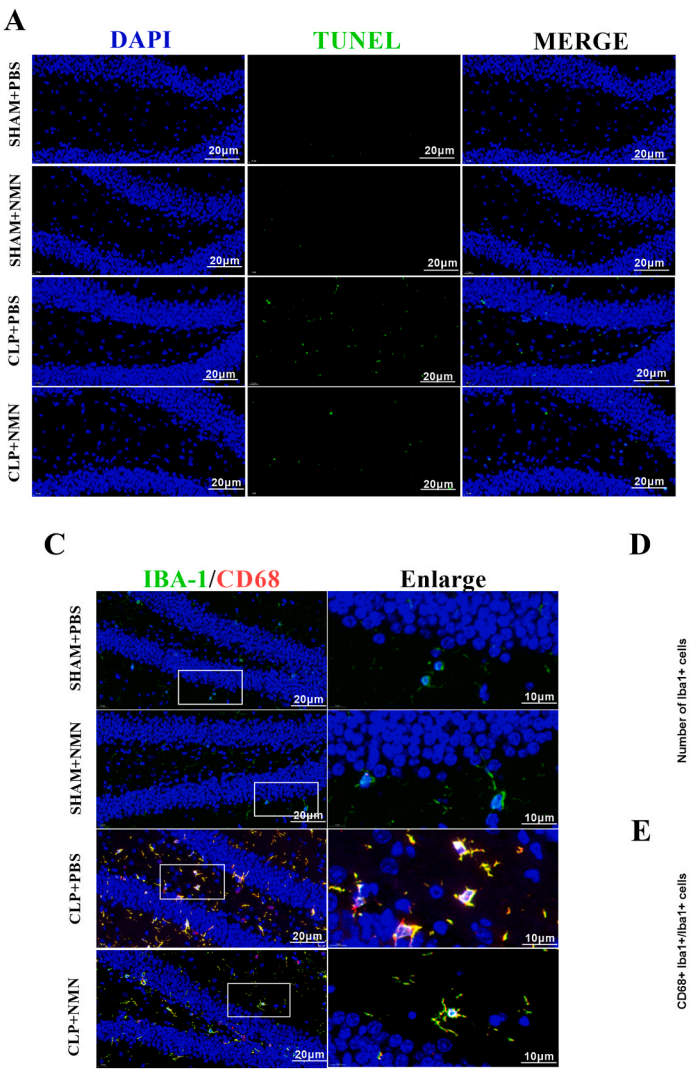

Fig. 4. NMN attenuated apoptosis and suppressed the activation of microglia in the hippocampus regions of septic mice. **(A, B)** Representative immunofluorescent staining images and quantification of TUNEL (green) with DAPI (blue) in the DG region of hippocampus. Scale bar = 20 μm. **(C)** Representative immunofluorescent staining images of Iba1+ (green), $CD68^{+}$ (red) with DAPI (blue) in the DG region of hippocampus. Scale bar = 20 μm. **(D, E)** Statistical diagram of the number of Iba1+ microglia cells and the ratio of $CD68^{+}$ Iba1+ cells/Iba1+ cells in the DG region of hippocampus. Tukey post-hoc test following a two-way ANOVA was used. The values were presented as mean ± SD (***$p < 0.001$, n = 3 or 6 for each group).

acetylation level of protein (Fig. 1B–E). Since it had been reported that SIRT1/PGC-1α could modulate the activity of p38 MAPK [17] and NF-κB [43], we detected the phosphorylation level of p38 and p65. In accordance with the total acetylation level, the phosphorylation levels of both P38 and P65 were significantly enhanced in CLP mice (Fig. 1F–H).

3.2. NMN rescued sepsis-induced depletion of NAD+/SIRT1 pathway, and inhibited inflammatory responses in the septic hippocampus

Since NMN is an intermediate for NAD + generation, we sought to investigate the role of NMN administration in the NAD+/SIRT1 pathway and neuroinflammation in septic mice. The experimental timeline was shown in Fig. 2A and the chemical formula of NMN was shown in Fig. 2B. As shown in Fig. 2, our results showed that NMN supplementation could significantly increase the level of NAD+ in the hippocampus of CLP mice at 24 h (Fig. 2C), but also restore the level of NAD+ in the hippocampus to a certain extent within 72 h (Fig. S4). And NMN treatment could increase the expressions of SIRT1 and PGC-1α in the hippocampus of septic mice (Fig. 2D, E, G). NMN could also reduce the increased level of total lysine acetylation induced by LPS to some extent. (Fig. 2D, I). Moreover, western blots showed that NMN decreased the phosphorylation level of P65 and P38 in the septic hippocampus (Fig. 2J-L). In order to further explore the mechanism by which NMN enhances the expression of SIRT1/PGC-1α, we used RT-qPCR to detect mRNA levels of SIRT1/PGC-1α in the hippocampus of CLP mice (Fig. 2F, H), results showed they were significantly decreased, while the supplementation of NMN could restore the expression to some extent, suggesting that the mechanism of NMN may be involved in the transcription level.

3.3. NMN mitigated memory impairment in septic mice

Since NMN reversed the depletion of NAD+/SIRT1 pathway and inhibited sepsis-induced neuroinflammation, we next investigate whether NMN improved memory function and the survival rate of septic mice. To investigate the effect of NMN on the overall survival rate of mice, CLP mice were intraperitoneally injected with NMN (500 mg/kg) and observed for 7 days. We found that NMN treatment could not improve the survival rate of the CLP mice. (Fig. 3A). In addition, Morris water maze and fear conditioning test were used to explore the effect of NMN on memory impairment caused by CLP. In the Morris water maze, our study found that the escape latency gradually decreased over the four days of training in all groups (Fig. 3B). The CLP group showed longer escape latencies in the training days, and spent shorter time and had fewer crossings in the target quadrant on the probe trial day than the sham group, while NMN treatment could restore them to some extent (Fig. 3C–E). In addition, the swimming speed was similar among the four groups (Fig. 3F). In the fear conditioning test, the freezing time in response to the context (Fig. 3G) and tone stimulation (Fig. 3H) in the CLP group was significantly shortened than in the sham group within 3

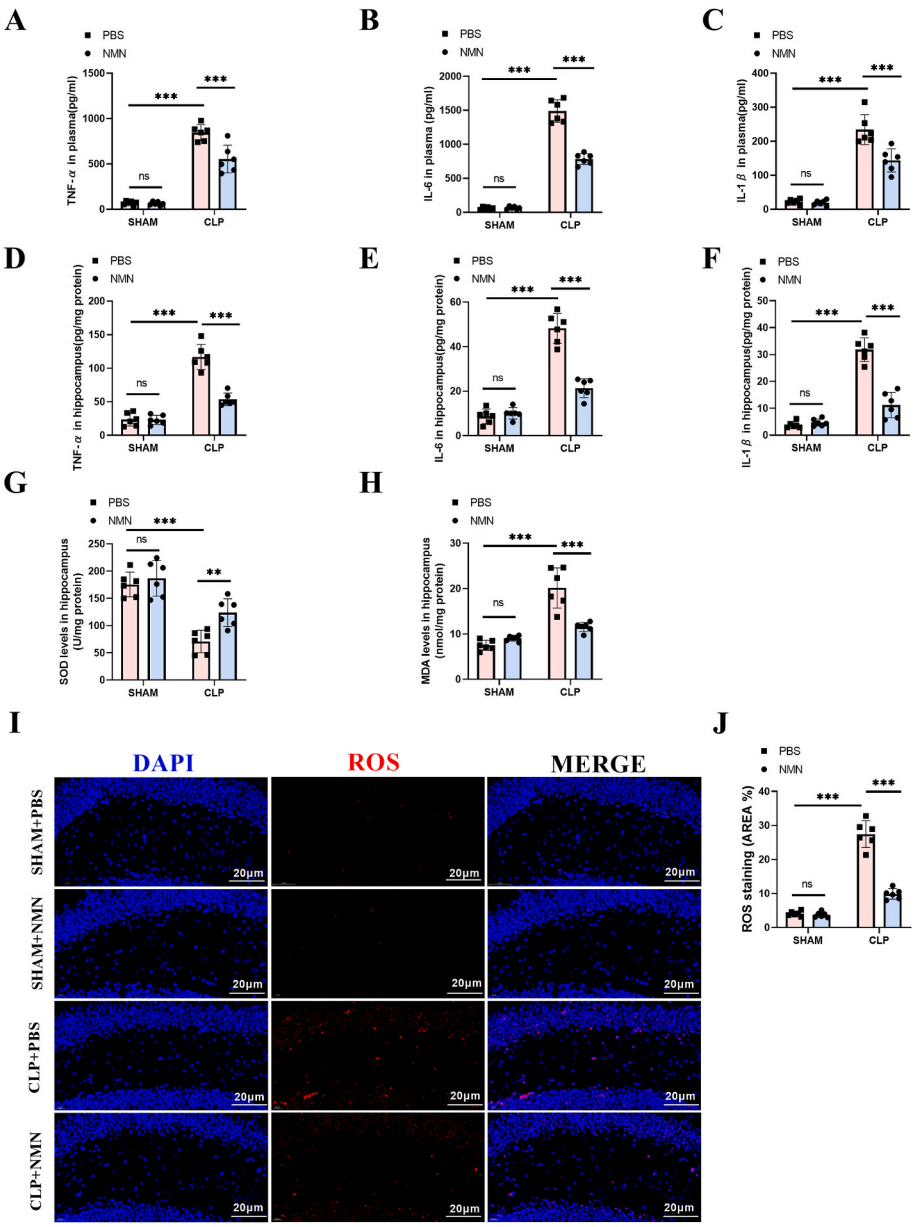

Fig. 5. NMN reduced the levels of inflammatory factors in the plasma and hippocampus, and attenuated the oxidative stress in hippocampus of septic mice at 24 h after surgery. **(A)** Plasma TNF-α. **(B)** Plasma IL-6. **(C)** Plasma IL-1β. **(D)** TNF-α in hippocampus. **(E)** IL-6 in hippocampus. **(F)** IL-1β in hippocampus. **(G)** The SOD activity. **(H)** MDA content. **(I, J)** Representative images and quantification of ROS immunostaining in the hippocampus region. Scale bar = 20 μm. Tukey post-hoc test following a two-way ANOVA was used. The values were presented as mean ± SD (**p < 0.01, ***p < 0.001, n = 6 for each group).

min, while NMN treatment recovered the freezing time in the CLP mice. Therefore, NMN may play a role in improving memory impairment induced by CLP.

3.4. NMN ameliorated apoptosis and suppressed the activation of microglia in the hippocampus regions of sepsis mice

The TUNEL assessment was performed to investigate the effect of NAD + on sepsis-induced apoptosis in the hippocampus region. The results demonstrated that the apoptosis rate in the hippocampus of CLP mice were significantly higher than in that of sham-operated mice, while NMN administration reduced apoptotic cells significantly (Fig. 4A and B). Microglial activation is a hallmark of neuroinflammation in SAE [4]. In order to explore the role of NMN in sepsis-induced microglial activation, IBA-1 and CD68 in combination was used as the markers for activated microglia [44,45]. The results showed that the activated microglial cells in the hippocampus of CLP mice were significantly increased, while NMN treatment significantly decreased the number of activated microglia (Fig. 4C–E), suggesting that NMN may inhibit neuroinflammation by inhibiting microglial activation.

3.5. NMN inhibited the neuroinflammation and oxidative stress in the hippocampus of SAE mice

Considering the contribution of inflammatory response and oxidative stress in the pathogenesis of SAE, we detected the levels of inflammatory cytokines and oxidative levels in the hippocampus of septic mice to further explore the anti-inflammatory and anti-oxidative effects of NMN. The results showed that the levels of inflammatory cytokines, including IL-6, IL-1β and TNF-α, in both of the hippocampus and serum of sepsis mice were significantly increased, while NMN treatment decreased the levels of IL-6, IL-1β and TNF-α significantly (Fig. 5A–F, S4). Similarly, the oxidative stress, as shown by the increased level of MDA and ROS, and reduced activity of SOD, was enhanced in the hippocampus of CLP mice, while NMN treatment attenuated the oxidative stress significantly (Fig. 5G–J).

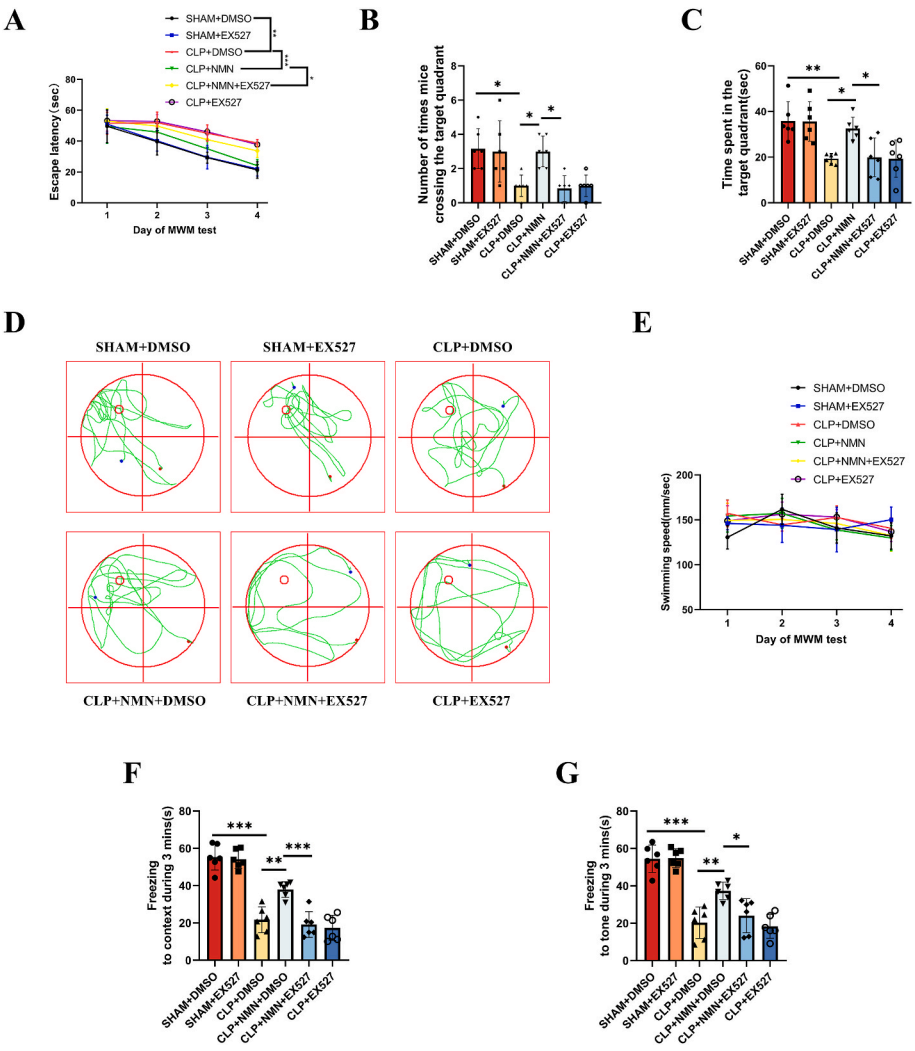

Fig. 6. The SIRT1 inhibitor, EX-527, reversed the protective effects of NMN against the memory impairment. (A) Escape latency time. **(B)** Number of crossings over the target quadrant in the Morris water maze beginning on day 18 after CLP. **(C)** Time spent in the target quadrant. **(D)** Representative swimming paths on the test day. The smaller red circle indicates the location of the training platform, which was removed during the test. **(E)** swimming speed in the Morris water maze. **(F)** The freezing time in response to the context in the fear conditioning test. **(G)** The freezing time in response to the tone in the fear conditioning test. Tukey post-hoc test following a two-way ANOVA was used in (A) and (E), one-way ANOVA was used in other figures. The values were presented as mean ± SD (*p < 0.05, **p < 0.01, ***p < 0.001, n = 6 in each group for Morris water maze and fear conditioning tests).

3.6. EX-527, an SIRT1 inhibitor, counteracted the protective effect of NMN against SAE

In order to further confirm that the protective effect of NMN is associated with SIRT1, we used EX-527, a selective inhibitor of SIRT1, to block SIRT1 pathway in CLP mice treated with NMN. Interestingly, in CLP mice treated with NMN and EX-527 simultaneously, the escape latencies in the training days were elevated (Fig. 6A). In addition, the time spent and crossings in the target quadrant on the test day (Fig. 6B–D) as well as the freezing time to context and tone stimulation (Fig. 6F and G) were reduced to a similar level to CLP mice treated with PBS. And the swimming speed was similar among the six groups.

The reduced rate of TUNEL positive cells and decreased activated microglial cells in the hippocampus of NMN-treated CLP mice were also reversed by EX-527 (Fig. 7A–E). Similarly, NMN-associated upregulation of SIRT1 and PGC-1α, and the inhibition of lysine acetylation, oxidative stress and proinflammatory load of cytokines in CLP mice were all reversed by the SIRT1 blocking using EX-527 (Fig. 8A-R). In addition, immunofluorescence co-staining of iba-1 and SIRT1 was performed in the hippocampus of mice, and it was found that the positive rate of SIRT1 in microglia cells of CLP mice was significantly decreased, while NMN supplementation could increase the expression of SIRT1 in microglia cells, and EX-527 partially inhibited the effect of NMN (Fig. S5). These results suggested that the protective effects of NMN against neuroinflammation, oxidative stress and memory impairment in CLP mice were associated with SIRT1 activity.

3.7. NMN ameliorated LPS-induced BV-2 activation by activating NAD+/SIRT1 pathway

Since microglia plays a central role in the neuroinflammation during SAE, we performed the *in vitro* experiments to investigate the anti-inflammatory and anti-oxidative effects of NMN in activated BV-2 cells. The results showed that LPS significantly reduced the levels of NAD + while promoting the production of proinflammatory cytokines and inducing oxidative stress in BV-2 cells, while NMN supplement restored the inflammatory and oxidative load induced by LPS (Fig. 9A–H). Moreover, LPS-induced depletion of SIRT1, PGC-1α at both the protein and mRNA levels, as well as the enhanced total acetylation of proteins and phosphorylation of P38 and P65 were attenuated by the supplement of NMN (Fig. 9I-L). The above results motivated us to find out how NMN affects SIRT1 at the transcriptional level in BV-2 cells. To do this, we detected the gene silence-associated promoter methylation of SIRT1. The results showed that the methylation level of SIRT1 promoter was increased in LPS stimulated cells, while the methylation level of SIRT1 was mitigated by NMM (Fig. 9M – O). S-adenosyl methionine (SAM) is an important metabolic intermediate and is the main biological methyl donor in most transmethylation [46], so we further examined the levels of SAM in BV-2 cells and found that SAM levels increased under LPS stimulation, and the supplement of NMN depleted it (Fig. S6A). Increased amount of niacinamide produced when NAD+ is decomposed during SIRT1 deacetylation reaction. Niacinamide could be quickly recycled or converted into methyl-nicotinamide so as not to inhibit NAD

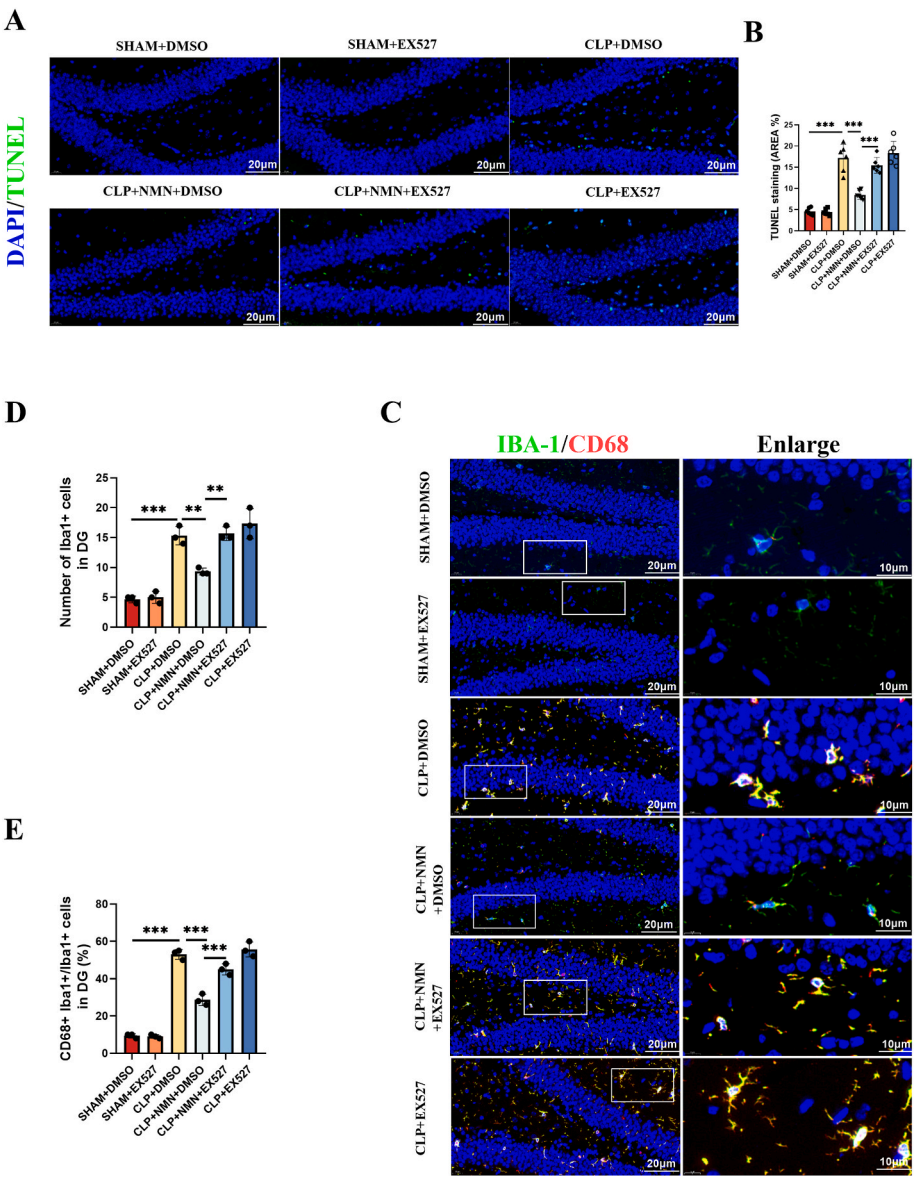

Fig. 7. The SIRT1 inhibitor, EX-527, reversed the protective effects of NMN against apoptosis and microglial activation. (A, B) Representative immunofluorescent staining images and quantification of TUNEL (green) with DAPI (blue) in the DG region of hippocampus. Scale bar = 20 μm. **(C)** Representative immunofluorescent staining images of Iba1+ (green), $CD68^{+}$ (red) with DAPI (blue) in the DG region of hippocampus. Scale bar = 20 μm. **(D, E)** Statistical diagram of the number of Iba1+ microglia cells and the ratio of $CD68^{+}$ Iba1+ cells/Iba1+ cells in the DG region of hippocampus. Tukey post-hoc test following one-way ANOVA was used. The values were presented as mean ± SD (*$p < 0.05$, **$p < 0.01$, ***$p < 0.001$, n = 3 or 6 for each group).

+ dependent enzymes. If recycling is limited (maybe by downregulation of NAMPT) [47], nicotinamide methyltransferase (NNMT) will be the limiting step of NAM conversion, and needs SAM as donor. If the pool of this methyl donor is depleted, other methylation reactions, such as promoter methylation could be reduced [48]. To test this hypothesis, we further performed experiments using NAM with the same concentration as NMN for verification *in vitro*, and found that the supplementation of NAM could lead to the similar results in the vitro model as NMN. NAM supplementation could effectively restore NAD + level changes induced by LPS, and play an anti-inflammatory and antioxidant stress role (Figs. S6B–J).

EX-527 and the SIRT1 knockdown experiments were performed to observe if the anti-inflammatory and anti-oxidative effects of NMN were related to SIRT1 activity. Again, the upregulation of SIRT1 and PGC-1α by NMN and the inhibition of NMN against production of proinflammatory cytokine, oxidative stress, acetylation level of total protein and phosphorylation level of P38 and P65 were all reversed by EX-527 and SIRT1 knockdown (Fig. 10, S7).

4. Discussion

SAE is an acute progressive brain disorder with systemic inflammatory response syndrome (SIRS) characterized by the absence of CNS infection. It is often associated with increased mortality [49]. Despite the high number of SAE-related deaths, there is still a lack of effective treatment for SAE. In the present study, we showed that NAD+/SIRT1 pathway was depleted in the hippocampus of CLP mice. The administration of NMN restored the NAD+/SIRT1 activity and improved the memory impairment of CLP mice to some extent. NMN also ameliorated CLP-induced apoptosis, neuroinflammation and oxidative stress in the hippocampus region of septic mice. The protective effect of NMN against SAE *in vivo* were almost completely reversed by the SIRT1 inhibitor, EX-527. Similar results were also observed *in vitro* using the BV-2 cells stimulated with LPS. NMN treatment attenuated LPS induced depletion of SIRT1 and PGC-1α, and alleviated inflammatory and oxidative load in BV-2 cells, while EX-527 or SIRT1 knockdown reversed the protective effects of NMN to a certain extent *in vitro* as well (Fig. 11).

NAD+ is an important metabolite, which is closely related to genome stability, mitochondrial homeostasis and adaptive stress response. Aging may lead to context- and tissue-dependent NAD + reduction in both

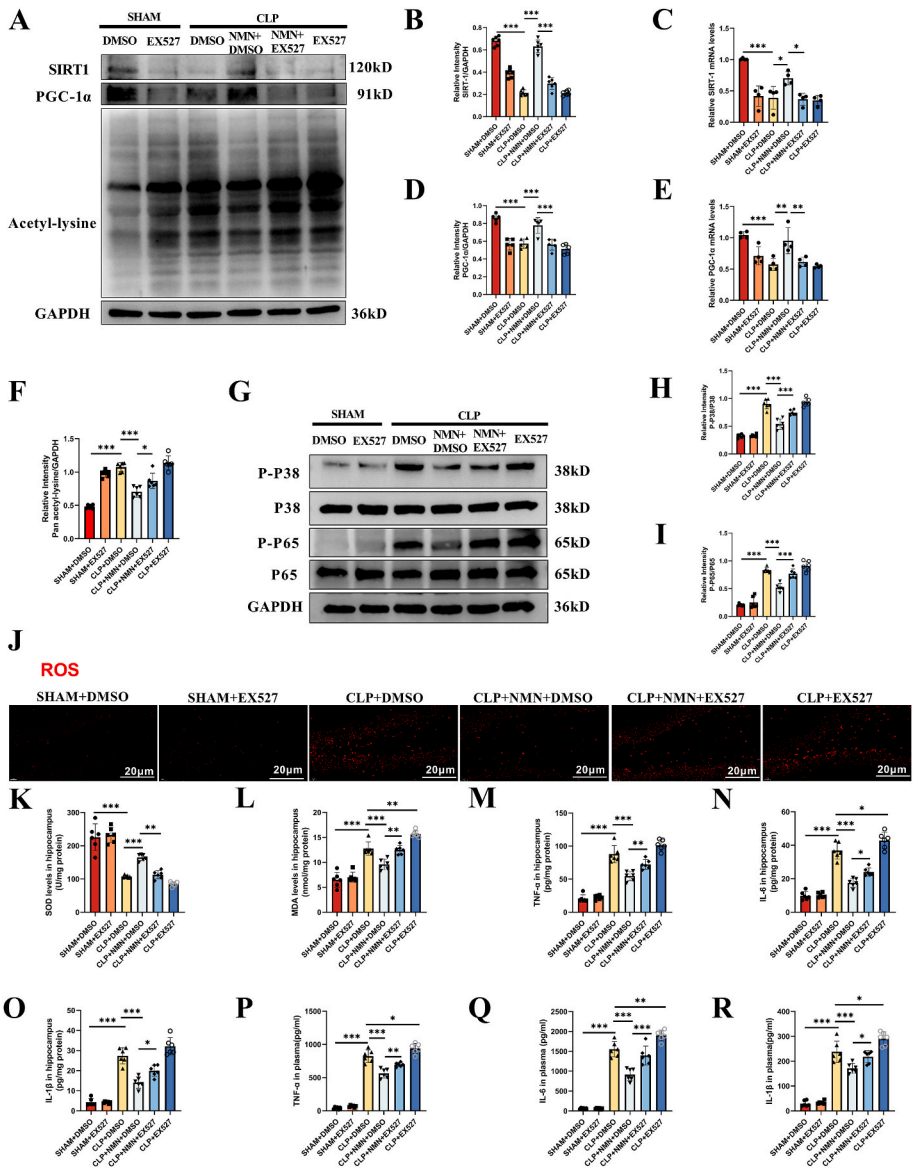

Fig. 8. EX-527 reversed the protective effects of NMN against the oxidative stress and inflammatory responses. (A–F) Expression levels and the relative quantification of SIRT1 and PGC-1α, and the acetylation level of lysine in hippocampus. **(G–I)** Phosphorylation and the relative quantification of P38 and P65 in hippocampus. **(J)** Representative images of ROS immunostaining in hippocampus. Scale bar = 20 μm. **(K)** The activity of SOD in hippocampus. **(L)** MDA content in hippocampus. **(M)** TNF-α in hippocampus. **(N)** IL-6 in hippocampus. **(O)** IL-1β in hippocampus. **(P)** Plasma TNF-α. **(Q)** Plasma IL-6. **(R)** Plasma IL-1β. Tukey post-hoc test following one-way ANOVA was used. The values were presented as mean ± SD (*p < 0.05, **p < 0.01, ***p < 0.001, n = 4 or 6 for each group).

human and mouse brain tissues [50–52], and reduced NAD + levels lead to impaired mitochondrial and microglial function after acute brain injury and in neurodegenerative diseases [33]. Multiple NAD + -dependent enzymes are involved in synaptic plasticity and neuronal stress resistance [53]. NAD+ is a substrate of sirtuin enzymes, which are important epigenetic regulators involved in metabolism, genome stability maintenance and immune response. SIRT1 exists mainly in the nucleus to deacetylate histone and serve as an effective protective factor for neurons under oxidative stress [54]. SIRT1 could upregulate mitochondrial biogenesis, gluconeogenesis and other metabolic processes by activating PGC-1α via deacetylation. One of the main functions of PGC-1α in mitochondria is to reduce ROS production by regulating the expression of many enzymes that antagonize ROS [55]. Moreover, PGC-1α acetylation is closely related to its co-transcriptional activity, when PGC-1α acetylation occurs, its transcriptional activity decreases, while SIRT1 could deacetylate PGC-1α [56]. A large number of studies had also shown that SIRT1 plays an important protective role in sepsis, which is not only found in some organs such as liver, lung and kidney, but also has a protective effect on sepsis-induced brain injury. And SIRT1 expression was significantly reduced in these CLP mice [57,58]. The same result was found in our experiment. Recently, it has been reported that epigenetic changes could lead to decreased expression of SIRT1 through its DNA methylation, resulting in oxidative damage to cells [59].

Our data showed that CLP and LPS induced depletion of NAD+, SIRT1 and PGC-1α in the hippocampus *in vivo* and in BV2 cells *in vitro*, suggesting that NAD + supplementation might improve sepsis-associated encephalopathy. Several studies have demonstrated that NMN was protective against acute or chronic inflammation. Liu et al. reported that NMN could inhibit PGE2 synthesis by reducing the expression of COX-2 in macrophages, consequently, it alleviated the endotoxin-induced inflammation and oxidative stress [60]. Another study reported that NMN administration prevented diabetes-induced cognitive impairment and hippocampal neuron loss by up-regulating the NAD + -dependent SIRT1 signaling pathway and down-regulating the acetylation pathway in the hippocampus of diabetic rats [61]. In addition, it had been found that NAD + concentration is significantly reduced during acute kidney injury, and NMN is used as a supplement of NAD + to restore its level, NAD + improves endotoxin-induced acute kidney injury in a SIRT1-dependent manner through GSK-3β/Nrf2 signaling pathway [62]. However, the role of NMN in SAE is rarely reported. It has been reported that of the NMN administration via

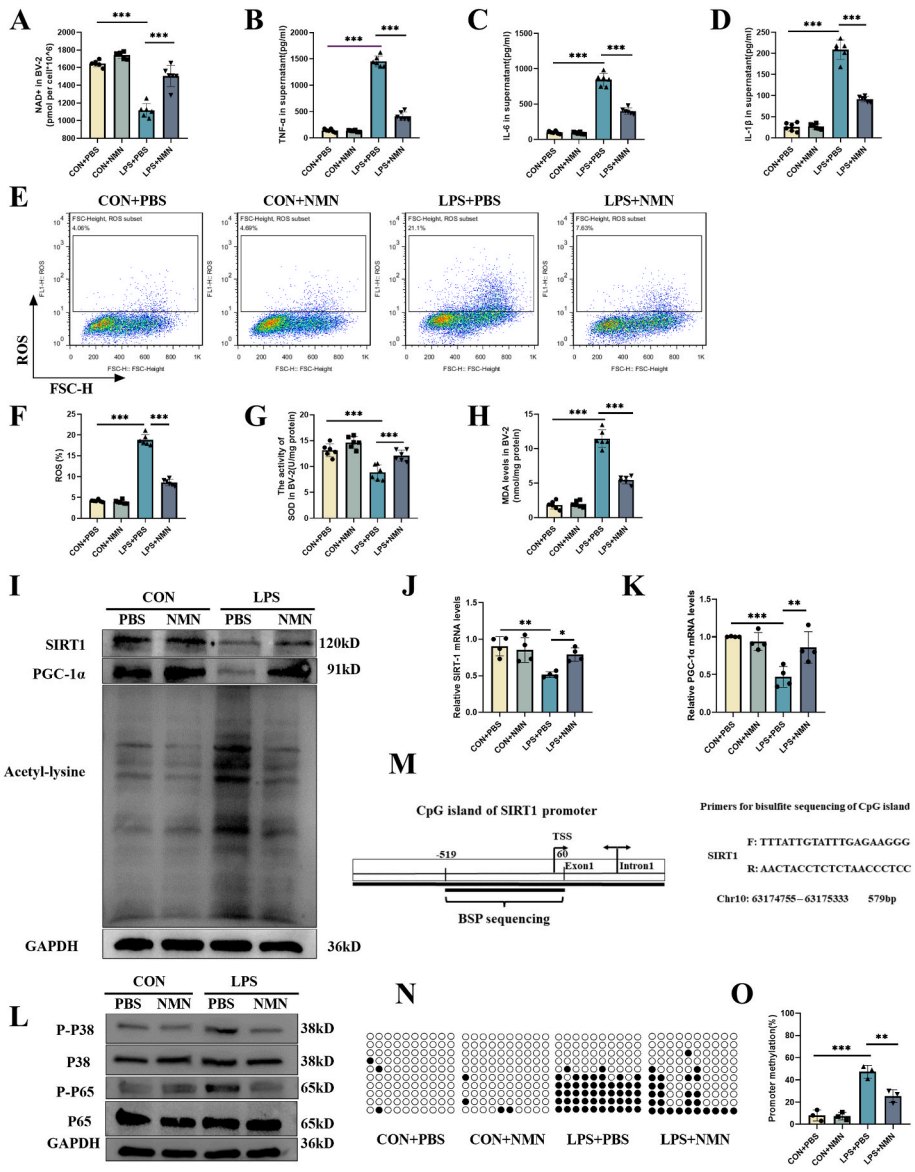

Fig. 9. NMN ameliorated the inflammatory and oxidative responses in BV-2 cells stimulated with LPS for 24 h *in vitro*. (A) NAD+ in BV-2. **(B)** Supernatant TNF-α. **(C)** Supernatant IL-6. **(D)** Supernatant. IL-1β. **(E, F)** The ROS level of BV-2 as detected by flow cytometry. **(G)** The SOD activity of BV-2. **(H)** MDA content in BV-2. **(I)** Protein expression of SIRT1, PGC-1α, and acetylation level of lysine in BV-2. **(J–K)** mRNA expression of SIRT1, PGC-1α in BV-2. **(L)** Phosphorylation of P38 and P65. **(M)** CpG island of SIRT1 gene with location and sequence of methylation-specific primers. **(N)** Methylation status of cytosine residues in SIRT1 promoter. **(O)** BSP assay identified the hypermethylation status of SIRT1. Each circle represents a CG site, the black circles represent methylation and the white circles represent unmethylation. Each row represents a sequencing result of a TA clone in a sample. Tukey post-hoc test following one-way ANOVA was used. The values were presented as mean ± SD (*p < 0.05, **p < 0.01,***p < 0.001, n = 3–6 for each group).

intraperitoneal injection could facilitate the synthesis of NAD+ and effectively restore the level of NAD+ in brain regions such as hippocampus [63,64]. In our study, it was found that NMN supplementation increased NAD + concentration, and additionally, it could upregulate SIRT1 and PGC-1α protein levels to a certain extent. This result is similar to the previous results of other scholars, such as Das Abhirup et al., who found the treatment of HUVECs with NMN could increase SIRT1 protein level [65]. In addition, Chandrasekaran et al. found that NMN treatment prevented the diabetes-induced decrease in both SIRT1 and PGC-1α, and promoted deacetylation of proteins, moreover, the diabetes-induced memory deficits were prevented by NMN [61].

Although the present and previous studies have found that SIRT1 expression is reduced during inflammatory responses and oxidative damage [57,66], but the underlying mechanism of NMN regulates SIRT1 expression was not well elucidated. In our present study, the expression of SIRT1 and PGC-1α mRNA was also decreased in CLP mice or LPS-stimulated cells, and this change was alleviated by NMN treatment. This indicates that NMN not only activates SIRT1, but also upregulate the levels of SIRT1 and PGC-1α at the transcription level. The mechanism how NMN regulate SIRT1 expression is unclear and the regulation of DNA methylation may be involved. DNA methylation is one of the epigenetic modifications. Many studies have shown that DNA methylation plays an important role in gene expression, hypermethylation in distal or proximal gene regulatory elements, such as transcriptional start sites (TSS), is often associated with the transcriptional repression of nearby genes [67,68]. We examined SIRT1 gene by BSP sequencing, and found that the methylation level of SIRT1 promoter was increased in LPS stimulated cells and reversed by NMM. DNA methyltransferase (DNMT) was reported to be inhibited by SIRT1 agonist, resveratrol, and inhibition of methylation was associated with enhanced expression of SIRT1 [59,69]. Therefore, we speculated that there might be a positive-feedback pathway involved in the regulation of SIRT1 expression via methyltransferases, and when NMN activate SIRT1, it might also increase SIRT1 expression by inhibiting DNA methylation as the positive-feedback mechanism. On the other hand, we found that LPS challenge resulted in SAM elevation in BV-2 cells, in contrast to the reduced level of NAD+. The dysregulation of NMN/NAD+/NAM cycle in the hippocampus of CLP mice or LPS-challenged BV-2 cells might be associated with altered NAM metabolism. The key enzymes, NAMPT, involved in the transformation of NAM to NMN might be down-regulated during CLP. And then NAM would be converted to methyl-nicotinamide by nicotinamide methyltransferase (NNMT), which required SAM as a donor of methyl. This process might lead to the depletion of SAM and the reduction of

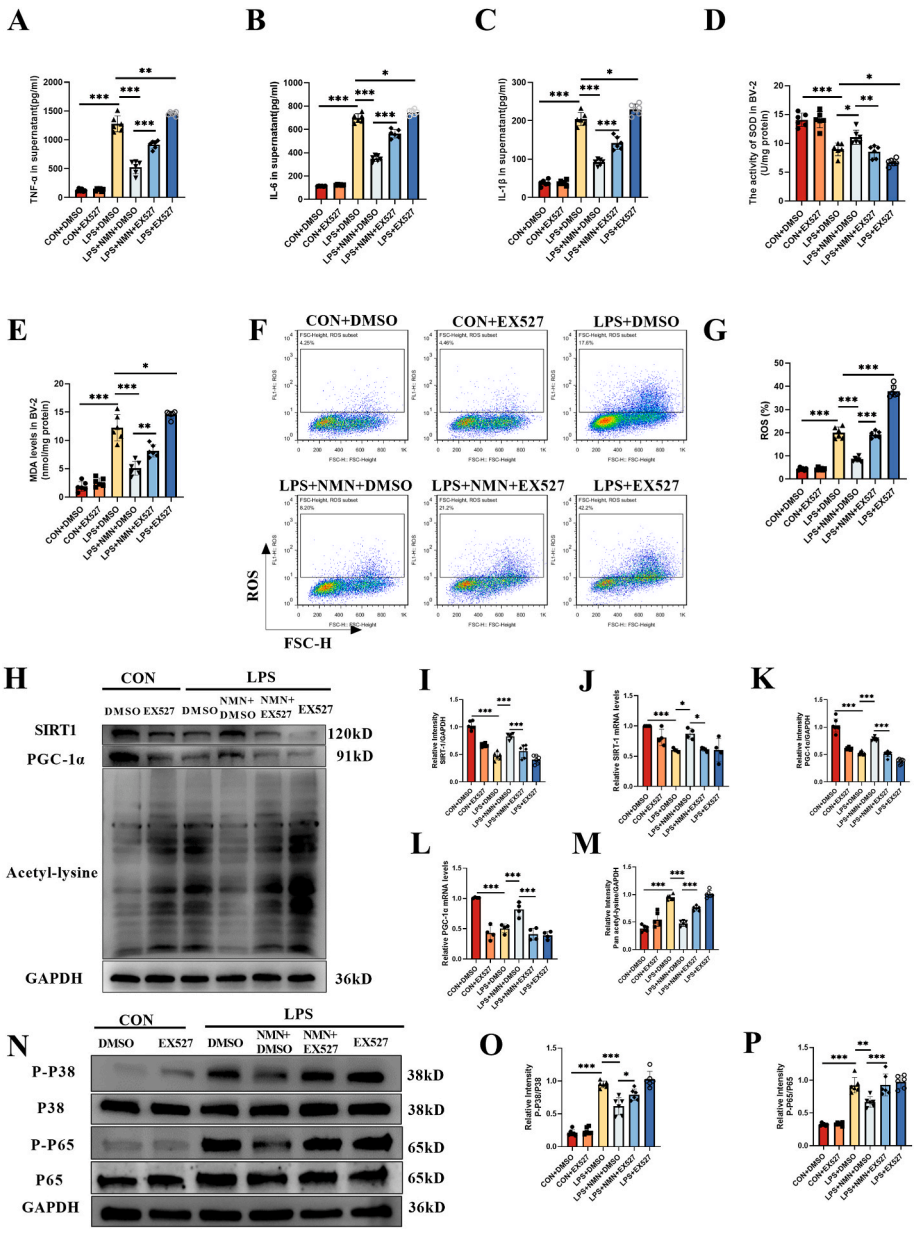

Fig. 10. EX-527 reversed the protective effect of NMN against inflammaroty and oxidative responses to LPS in BV-2 cells. (A) Supernatant TNF-α. **(B)** Supernatant IL-6. **(C)** Supernatant IL-1β. **(D)** The SOD activity in BV-2. **(E)** MDA content in BV-2. **(F, G)** The level of ROS in BV-2 as detected by flow cytometry. **(H–M)** Expression and the relative quantification of SIRT1, PGC-1α, and acetylation level of lysine in BV-2. **(N–P)** Phosphorylation and the relative quantification of P38 and P65. Tukey post-hoc test following one-way ANOVA was used. The values were presented as mean ± SD (*p < 0.05, **p < 0.01, ***p < 0.001, n = 4 or 6 for each group).

promoter methylation. Therefore, LPS-challenge might enhance the methylation of SIRT1 and PGC-1α, while NMN supplement reversed these changes and increased the expression of SIRT1 and PGC-1α.

Although we provide evidence for a role of SIRT1 in ameliorating oxidative stress, inflammatory response, and cell death in SAE, we could not rule out a SIRT1-independent effect. The raised expression of NAMPT, involving in the NAD + salvage pathway as the rate-limiting enzyme, and indole-2,3-dioxygenase 1 (IDO1), mediating NAD + de novo synthesis pathways, which might be required for the maintenance of depleted NAD+ and to supply the production of pro-inflammatory factors in sepsis. The supplementation of NAD + precursor could restore the overexpression of genes involved in these pathways, also affect the tryptophan and kynurenine metabolic pathways during NAD + de novo synthesis, and improve cellular immunomodulatory capacity [30,70,71]. Poly-adenosine diphosphate-ribose polymerases (PARPs) is a nuclear chromatin-associated protein, which function as an enzyme, could catalyze the transfer of ADP-ribose units from its substrate NAD + covalently to itself and other nuclear chromatin-associated proteins. PARPs are critical DNA repair enzymes, and have an important impact on transcriptional activation of NF-κB and systemic inflammatory processes as a coactivator of NF-κB [72,73]. The inflammatory response leads to DNA damage, which in turn activates PARPs, and the overactivation of PARPs could lead to the depletion of NAD+ [74,75]. We speculate that the anti-inflammatory and antioxidant stress induced by NMN may be a non-specific reaction. It may be that the internal environment tends to improve just because the level of NAD+ is restored, which may inhibit the overactivation of PARPs. Considering the role of PARPs, NAD + de novo synthesis and salvage pathways in immune response, we speculated that in addition to SIRT1, these factors might be the potential mechanisms in the improvement of SAE by NMN. Moreover, the mechanism of how NMN is absorbed into cells is not entirely clear. It has been reported that NMN is converted extracellularly to NR, then NR will be transported into cells and reconverted to NMN [76]. Another study reported that NMN could directly enter cells via Slc12a8 transporter [77]. However, there has been controversy around these mechanisms.

Microglia is the resident immune cell in the brain tissue. In SAE, microglia could be recruited to inflammation regions by the local

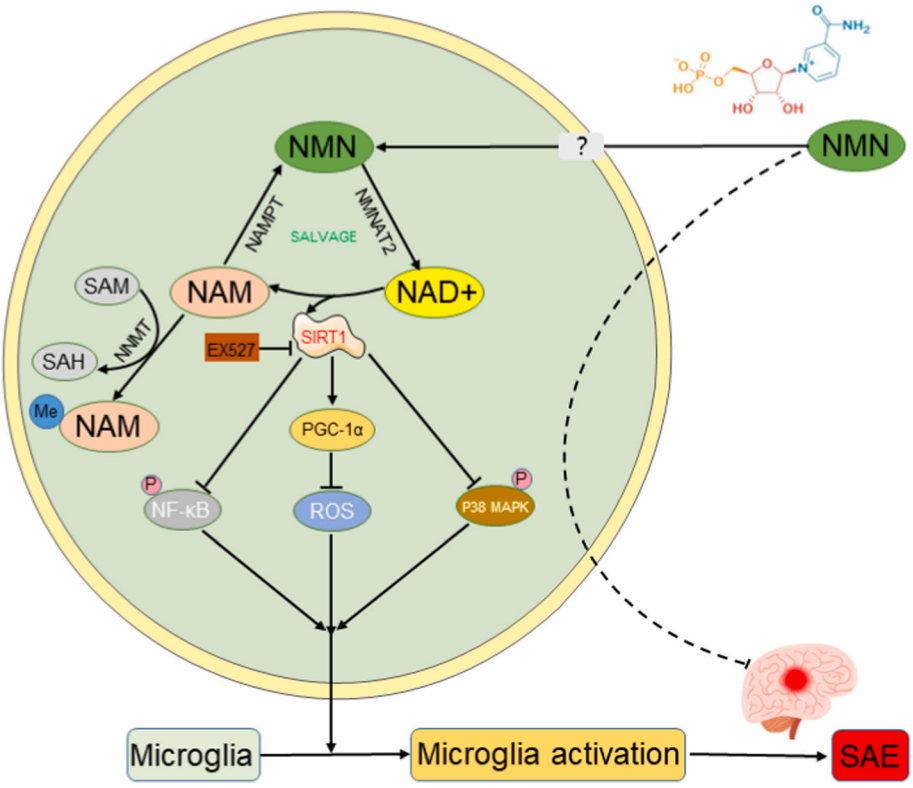

Fig. 11. Graphic summary. The administration of NMN restores the NAD+/SIRT1 activity in sepsis-associated encephalopathy. NMN upregulates PGC-1α, inhibits the acetylation of proteins and phosphorylation of P38 MAPK and P65 NF-κB pathways dependent in the SIRT1 activity. Sepsis-induced apoptosis, microglia activation, neuroinflammation and oxidative stress in the hippocampus regions of septic mice are attenuated by NMN supplement, which improves the memory impairment of septic mice.

produced proinflammatory mediators, to ensure the normal brain function through the secretion of protease, nitric oxide, reactive oxygen intermediates and proinflammatory cytokines. However, overactivation of microglia may result in overwhelming inflammatory responses [78], which exacerbate brain dysfunction such as memory impairment and even lead to death [79]. Therefore, the activation of microglia and the release of inflammatory cytokines play a central role in the development of SAE [80]. The activation of MAPK and NF-κB promotes the expression of interleukin-1β (IL-1β), tumor necrosis factor-α (TNF-α), and interleukin-6 (IL-6), which induces inflammation and leads to mitochondrial dysfunction [81]. Upregulation of SIRT1 had been reported to inhibit P38 MAPK and NF-κB signaling pathways, and enhance oxidative metabolism and inflammation resolution [43,82,83]. Another study had shown that SIRT1 inhibits the NF-κB signaling pathway through the deacetylation of the NF-κB subunit p65 at lysine 310, acting as a negative regulator to control microglial overactivation [84]. Our experimental results showed that abdominal sepsis induced hippocampal microglial activation, apoptosis, and elevated load of neuroinflammation and oxidative stress. NMN could alleviate these changes and improved the memory impairment of septic mice to a certain extent. Furthermore, our data demonstrated that SIRT1 inhibitor (EX-527) could weaken the therapeutic effects of NMN, indicating that NAD+/SIRT1 pathways might be involved in the mechanisms of the protective effect. However, we could not explain why EX-527 was able to reduce the expression of SIRT1 and PGC-1α, which was also observed in other studies [85,86]. Further studies might be required to clarify the exact role of EX-527 in SIRT1 expression and activity, which was beyond of our present study. And the use of siRNA transfection might provide additional evidence for the involvement of SIRT1 pathway in NMN activity against SAE.

There are several limitations in our study. First, we did not pay much attention on the development of sepsis regarding the general condition, systemic inflammation and impairment of other organs, because we want to focus more on the encephalopathy induced by sepsis. Further study might be performed to investigate the therapeutic role of NMN against sepsis. Second, we did not perform a dose-response experiment to identify the most suitable dose, and the dose was chosen in accordance with the references. Third, the method of NAD + quantification used in our study is consistent with the enzyme-based protocol described by Jia et al. [42]. However, during the using of ADH based NAD + assay, the oxidation products of acetaldehyde had been shown to interfere with the ADH if the generated acetaldehyde was not removed, possibly affected the accuracy of measurement within our acceptable limitation. Fourth, how NMN regulate the expression level of SIRT1 and PGC-1α should be further investigated, and our present study just proposed a speculation that methylation regulation might be involved. Fifth, drug administration at different time points could have different effects. It is generally considered that hyperinflammatory response is dominant in the early stage of sepsis, whereas immunosuppression is dominant in the later stage. We aimed to investigate the effect of NMN treatment in the acute proinflammatory response and organ dysfunction at the early stage of sepsis. On the other hand, it may also lead to compromised immunity. Generally, there are two groups of researchers. One of them suggest that reverse of immune dysfunction will enhance the clearance of pathogen and improve the prognosis. But the other think that early inhibition of inflammation will close the Pandora's box and block the formation of immunoparalysis [87,88]. In our present study, we administered NMN in CLP mice at a single time point similarly to other previous studies, because we want to first clarify the effect of NMN in CLP mice and then perform more pharmacological studies. Moreover, EX-527 administration at different time points of sepsis had different effects on the outcome of CLP mice. For example, EX-527 treatment could reverse endotoxin tolerance *in vivo* when administered at 24 h after sepsis, showed that all treated septic mice survived, whereas only 10% of treated septic mice survived at 0 h [89]. In our study, both NMN and EX-527 were administered immediately after surgery. It was a limitation of our study that we did not investigate the different effects of drug administration at different time points in our study, and we will keep on investigating this issue in future studies.

5. Conclusions

In conclusion, our present study demonstrated that NMN treatment could ameliorate sepsis-induced memory impairment, neuroinflammation and oxidative stress to a certain extent. The protective effect of NMN might be related to the enhanced NAD+/SIRT1 activity. Maintenance of SIRT1 activity by NMN was associated with upregulation of PGC-1α, inhibition of protein acetylation and phosphorylation of P38 MAPK and P65 NF-κB. Our data suggested that NMN might be a promising therapeutic strategy for SAE.

CRediT authorship contribution statement

Hui-ru Li, Qiang Liu and Cheng-long Zhu contributed equally to the article. Hui-ru Li carried out the majority of the experiments and analyzed the data. Qiang Liu and Cheng-long Zhu wrote the manuscript. Jia-feng Wang and Xiao-ming Deng designed the study protocol and revised the manuscript. Xiao-yang Sun, Chen-yan Sun, Chang-meng Yu and Peng Li assisted in performing the research. All authors approved the final version of the manuscript.

Declaration of competing interest

The authors declare that they have no known competing financial interests or personal relationships that could have appeared to influence the work reported in this paper.

Data availability

Data will be made available on request.

Acknowledgements

We gratefully acknowledge the financial support from National Natural Science Foundation of China (No. 82272214, 82072147), Sci-Tech Innovation 2030 Brain Science and Brain-Like Intelligence Technology Project (2022ZD0208100) and Shanghai Rising-Star Program (21QA1411800).

Abbreviations

CLP	cecal ligation and puncture
CNS	central nervous system
CD38	cluster of differentiation 38
DMSO	Dimethyl Sulfoxide
DMEM	dulbecco's modified eagle medium
DAPI	4′, 6-diaminidine-2-phenylindole
ELISA	Enzyme-linked immunosorbent assay
FoxO3a	forkhead boxO3a
FC	Fear Conditioning Test
FBS	fetal bovine serum
HDACs	histone deacetylases
IDO1	indole-2,3-dioxygenase 1
IL-1β	interleukin-1β
IL-6	interleukin-6
LPS	Lipopolysaccharide
MDA	malondialdehyde
NAD+	Nicotinamide adenine dinucleotide
NAM	nicotinamide
NAMPT	nicotinamide phosphoribosyl transferase
NMNATs	nicotinamide mononucleotide adenylyl transferases
NMN	β-Nicotinamide Mononucleotide
NF-κB p65	nuclear factor kappa B p65
NNMT	nicotinamide methyltransferase
PARP1	poly (ADP-Ribose) Polymerase 1
PGC-1α	peroxisome proliferator-activated receptor-gamma co-activator 1α
p38 MAPK	p38 mitogen-activated protein kinase
PBS	phosphate buffered saline
SAM	S-adenosyl methionine
SAH	S-adenosyl homocysteine
SAE	Sepsis-associated encephalopathy
SIRT1	Sirtuin 1
SOD	superoxide dismutase
TUNEL	Terminal Deoxynucleotidyl Transferase-mediated dUTP Nick End Labeling
TNF-α	umor necrosis factor-α

Appendix A. Supplementary data

Supplementary data to this article can be found online at https://doi.org/10.1016/j.redox.2023.102745.

References

[1] M. Singer, C.S. Deutschman, C.W. Seymour, M. Shankar-Hari, D. Annane, M. Bauer, R. Bellomo, G.R. Bernard, J.D. Chiche, C.M. Coopersmith, et al., The third international consensus definitions for sepsis and septic shock (Sepsis-3), JAMA 315 (2016) 801–810.
[2] K.E. Rudd, S.C. Johnson, K.M. Agesa, K.A. Shackelford, D. Tsoi, D.R. Kievlan, D. V. Colombara, K.S. Ikuta, N. Kissoon, S. Finfer, et al., Global, regional, and national sepsis incidence and mortality, 1990-2017: analysis for the Global Burden of Disease Study, Lancet 395 (2020) 200–211.
[3] T.E. Gofton, G.B. Young, Sepsis-associated encephalopathy, Nat. Rev. Neurol. 8 (2012) 557–566.
[4] A. Mazeraud, C. Righy, E. Bouchereau, S. Benghanem, F.A. Bozza, T. Sharshar, Septic-associated encephalopathy: a comprehensive review, Neurotherapeutics 17 (2020) 392–403.
[5] H.Y. Chung, J. Wickel, F.M. Brunkhorst, C. Geis, Sepsis-associated encephalopathy: from delirium to dementia? J. Clin. Med. 9 (2020).
[6] L. Rajman, K. Chwalek, D.A. Sinclair, Therapeutic potential of NAD-boosting molecules: the in vivo evidence, Cell Metabol. 27 (2018) 529–547.
[7] E. Migliavacca, S.K.H. Tay, H.P. Patel, T. Sonntag, G. Civiletto, C. McFarlane, T. Forrester, S.J. Barton, M.K. Leow, E. Antoun, et al., Mitochondrial oxidative capacity and NAD(+) biosynthesis are reduced in human sarcopenia across ethnicities, Nat. Commun. 10 (2019) 5808.
[8] E.F. Fang, S. Lautrup, Y. Hou, T.G. Demarest, D.L. Croteau, M.P. Mattson, V. A. Bohr, NAD(+) in aging: molecular mechanisms and translational implications, Trends Mol. Med. 23 (2017) 899–916.
[9] E. Verdin, NAD⁺ in aging, metabolism, and neurodegeneration, Science 350 (2015) 1208–1213.
[10] E. Fagerli, I. Escobar, F.J. Ferrier, C.W. Jackson, E.J. Perez-Lao, M.A. Perez-Pinzon, Sirtuins and cognition: implications for learning and memory in neurological disorders, Front. Physiol. 13 (2022), 908689.
[11] P. Wang, S. Zhang, S. Lin, Z. Lv, Melatonin ameliorates diabetic hyperglycaemia-induced impairment of Leydig cell steroidogenic function through activation of SIRT1 pathway, Reprod. Biol. Endocrinol. 20 (2022) 117.
[12] S. Gautam, L. Zhang, C. Lee, I. Arnaoutova, H.D. Chen, R. Resaz, A. Eva, B. C. Mansfield, J.Y. Chou, Molecular mechanism underlying impaired hepatic autophagy in glycogen storage disease type Ib, Hum. Mol. Genet. 32 (2) (2023) 262–275.
[13] M. Hao, C. Ding, X. Peng, H. Chen, L. Dong, Y. Zhang, X. Chen, W. Liu, Y. Luo, Ginseng under forest exerts stronger anti-aging effects compared to garden ginseng probably via regulating PI3K/AKT/mTOR pathway, SIRT1/NF-κB pathway and intestinal flora, Phytomedicine 105 (2022), 154365.
[14] G. Luo, L. Xiao, D. Wang, N. Wang, C. Luo, X. Yang, L. Hao, Resveratrol attenuates excessive ethanol exposure-induced β-cell senescence in rats: a critical role for the NAD(+)/SIRT1-p38MAPK/p16 pathway, J. Nutr. Biochem. 89 (2021), 108568.
[15] Y. Hao, Z. Ren, L. Yu, G. Zhu, P. Zhang, J. Zhu, S. Cao, p300 arrests intervertebral disc degeneration by regulating the FOXO3/Sirt1/Wnt/β-catenin axis, Aging Cell 21 (2022), e13677.
[16] T. Meng, W. Qin, B. Liu, SIRT1 antagonizes oxidative stress in diabetic vascular complication, Front. Endocrinol. 11 (2020), 568861.
[17] Z. Cui, X. Zhao, F.K. Amevor, X. Du, Y. Wang, D. Li, G. Shu, Y. Tian, X. Zhao, Therapeutic application of quercetin in aging-related diseases: SIRT1 as a potential mechanism, Front. Immunol. 13 (2022), 943321.
[18] Y. Wang, E. Xu, P.R. Musich, F. Lin, Mitochondrial dysfunction in neurodegenerative diseases and the potential countermeasure, CNS Neurosci. Ther. 25 (2019) 816–824.
[19] P.P. Su, D.W. Liu, S.J. Zhou, H. Chen, X.M. Wu, Z.S. Liu, Down-regulation of Risa improves podocyte injury by enhancing autophagy in diabetic nephropathy, Mil Med Res 9 (2022) 23.
[20] Z. Deng, M. Sun, J. Wu, H. Fang, S. Cai, S. An, Q. Huang, Z. Chen, C. Wu, Z. Zhou, et al., SIRT1 attenuates sepsis-induced acute kidney injury via Beclin1 deacetylation-mediated autophagy activation, Cell Death Dis. 12 (2021) 217.

[21] R. Nogueiras, K.M. Habegger, N. Chaudhary, B. Finan, A.S. Banks, M.O. Dietrich, T. L. Horvath, D.A. Sinclair, P.T. Pfluger, M.H. Tschöp, Sirtuin 1 and sirtuin 3: physiological modulators of metabolism, Physiol. Rev. 92 (2012) 1479–1514.

[22] J.M. Yuk, T.S. Kim, S.Y. Kim, H.M. Lee, J. Han, C.R. Dufour, J.K. Kim, H.S. Jin, C. S. Yang, K.S. Park, et al., Orphan nuclear receptor ERRα controls macrophage metabolic signaling and A20 expression to negatively regulate TLR-induced inflammation, Immunity 43 (2015) 80–91.

[23] W.Y. Kwon, G.J. Suh, K.S. Kim, Y.H. Kwak, Niacin attenuates lung inflammation and improves survival during sepsis by downregulating the nuclear factor-κB pathway, Crit. Care Med. 39 (2011) 328–334.

[24] M. Ye, Y. Zhao, Y. Wang, R. Xie, Y. Tong, J.D. Sauer, S. Gong, NAD(H)-loaded nanoparticles for efficient sepsis therapy via modulating immune and vascular homeostasis, Nat. Nanotechnol. 17 (2022) 880–890.

[25] H. Nadeeshani, J. Li, T. Ying, B. Zhang, J. Lu, Nicotinamide mononucleotide (NMN) as an anti-aging health product - promises and safety concerns, J. Adv. Res. 37 (2022) 267–278.

[26] O.K. Reiten, M.A. Wilvang, S.J. Mitchell, Z. Hu, E.F. Fang, Preclinical and clinical evidence of NAD(+) precursors in health, disease, and ageing, Mech. Ageing Dev. 199 (2021), 111567.

[27] T. Kiss, P. Balasubramanian, M.N. Valcarcel-Ares, S. Tarantini, A. Yabluchanskiy, T. Csipo, A. Lipecz, D. Reglodi, X.A. Zhang, F. Bari, et al., Nicotinamide mononucleotide (NMN) treatment attenuates oxidative stress and rescues angiogenic capacity in aged cerebromicrovascular endothelial cells: a potential mechanism for the prevention of vascular cognitive impairment, Geroscience 41 (2019) 619–630.

[28] T. Kiss, Á. Nyúl-Tóth, P. Balasubramanian, S. Tarantini, C. Ahire, A. Yabluchanskiy, T. Csipo, E. Farkas, J.D. Wren, L. Garman, et al., Nicotinamide mononucleotide (NMN) supplementation promotes neurovascular rejuvenation in aged mice: transcriptional footprint of SIRT1 activation, mitochondrial protection, anti-inflammatory, and anti-apoptotic effects, Geroscience 42 (2020) 527–546.

[29] Y. Jiang, Y. Deng, H. Pang, T. Ma, Q. Ye, Q. Chen, H. Chen, Z. Hu, C.F. Qin, Z. Xu, Treatment of SARS-CoV-2-induced pneumonia with NAD(+) and NMN in two mouse models, Cell Discov 8 (2022) 38.

[30] C. Cros, M. Margier, H. Cannelle, J. Charmetant, N. Hulo, L. Laganier, A. Grozio, M. Canault, Nicotinamide mononucleotide administration triggers macrophages reprogramming and alleviates inflammation during sepsis induced by experimental peritonitis, Front. Mol. Biosci. 9 (2022), 895028.

[31] J.F. Wang, Y.P. Wang, J. Xie, Z.Z. Zhao, S. Gupta, Y. Guo, S.H. Jia, J. Parodo, J. C. Marshall, X.M. Deng, Upregulated PD-L1 delays human neutrophil apoptosis and promotes lung injury in an experimental mouse model of sepsis, Blood 138 (2021) 806–810.

[32] S. He, Q. Gao, X. Wu, J. Shi, Y. Zhang, J. Yang, X. Li, S. Du, Y. Zhang, J. Yu, NAD(+) ameliorates endotoxin-induced acute kidney injury in a sirtuin1-dependent manner via GSK-3beta/Nrf2 signalling pathway, J. Cell Mol. Med. 26 (2022) 1979–1993.

[33] J. Yoshino, J.A. Baur, S.I. Imai, NAD(+) intermediates: the biology and therapeutic potential of NMN and NR, Cell Metabol. 27 (2018) 513–528.

[34] X. Zhuang, Y. Yu, Y. Jiang, S. Zhao, Y. Wang, L. Su, K. Xie, Y. Yu, Y. Lu, G. Lv, Molecular hydrogen attenuates sepsis-induced neuroinflammation through regulation of microglia polarization through an mTOR-autophagy-dependent pathway, Int. Immunopharm. 81 (2020), 106287.

[35] X. Wang, X. Hu, Y. Yang, T. Takata, T. Sakurai, Nicotinamide mononucleotide protects against beta-amyloid oligomer-induced cognitive impairment and neuronal death, Brain Res. 1643 (2016) 1–9.

[36] R.A. Salazar-Gonzalez, M.A. Doll, D.W. Hein, Arylamine N-acetyltransferase 1 activity is regulated by the protein acetylation status, Front. Pharmacol. 13 (2022), 797469.

[37] X.S. Zhang, Y. Lu, W. Li, T. Tao, W.H. Wang, S. Gao, Y. Zhou, Y.T. Guo, C. Liu, Z. Zhuang, et al., Cerebroprotection by dioscin after experimental subarachnoid haemorrhage via inhibiting NLRP3 inflammasome through SIRT1-dependent pathway, Br. J. Pharmacol. 178 (2021) 3648–3666.

[38] A.Y.O. Silva, A. Amorim É, M.C. Barbosa-Silva, M.N. Lima, H.A. Oliveira, M. G. Granja, K.S. Oliveira, P.M. Fagundes, R.L.S. Neris, R.M.P. Campos, et al., Mesenchymal stromal cells protect the blood-brain barrier, reduce astrogliosis, and prevent cognitive and behavioral alterations in surviving septic mice, Crit. Care Med. 48 (2020) e290–e298.

[39] C.V. Vorhees, M.T. Williams, Morris water maze: procedures for assessing spatial and related forms of learning and memory, Nat. Protoc. 1 (2006) 848–858.

[40] H. Cao, C. Zuo, Z. Gu, Y. Huang, Y. Yang, L. Zhu, Y. Jiang, F. Wang, High frequency repetitive transcranial magnetic stimulation alleviates cognitive deficits in 3xTg-AD mice by modulating the PI3K/Akt/GLT-1 axis, Redox Biol. 54 (2022), 102354.

[41] C.T. Zhu, D.M. Rand, A hydrazine coupled cycling assay validates the decrease in redox ratio under starvation in Drosophila, PLoS One 7 (2012), e47584.

[42] R. Jia, J. Du, L. Cao, W. Feng, Q. He, P. Xu, G. Yin, Application of transcriptome analysis to understand the adverse effects of hydrogen peroxide exposure on brain function in common carp (Cyprinus carpio), Environ. Pollut. 286 (2021), 117240.

[43] A. Kauppinen, T. Suuronen, J. Ojala, K. Kaarniranta, A. Salminen, Antagonistic crosstalk between NF-κB and SIRT1 in the regulation of inflammation and metabolic disorders, Cell. Signal. 25 (2013) 1939–1948.

[44] K.I. Mosher, R.H. Andres, T. Fukuhara, G. Bieri, M. Hasegawa-Moriyama, Y. He, R. Guzman, T. Wyss-Coray, Neural progenitor cells regulate microglia functions and activity, Nat. Neurosci. 15 (2012) 1485–1487.

[45] K.E. Hopperton, D. Mohammad, M.O. Trépanier, V. Giuliano, R.P. Bazinet, Markers of microglia in post-mortem brain samples from patients with Alzheimer's disease: a systematic review, Mol. Psychiatr. 23 (2018) 177–198.

[46] W. Yu, Z. Wang, K. Zhang, Z. Chi, T. Xu, D. Jiang, S. Chen, W. Li, X. Yang, X. Zhang, et al., One-carbon metabolism supports S-adenosylmethionine and histone methylation to drive inflammatory macrophages, Mol. Cell 75 (2019) 1147–1160. e1145.

[47] C. Tannous, G.W. Booz, R. Altara, D.H. Muhieddine, M. Mericskay, M.M. Refaat, F. A. Zouein, Nicotinamide adenine dinucleotide: biosynthesis, consumption and therapeutic role in cardiac diseases, Acta Physiol. 231 (2021), e13551.

[48] M.A. Eckert, F. Coscia, A. Chryplewicz, J.W. Chang, K.M. Hernandez, S. Pan, S. M. Tienda, D.A. Nahotko, G. Li, I. Blaženović, et al., Proteomics reveals NNMT as a master metabolic regulator of cancer-associated fibroblasts, Nature 569 (2019) 723–728.

[49] M.C. Kodali, H. Chen, F.F. Liao, Temporal unsnarling of brain's acute neuroinflammatory transcriptional profiles reveals panendothelitis as the earliest event preceding microgliosis, Mol. Psychiatr. 26 (2021) 3905–3919.

[50] L.R. Stein, S. Imai, Specific ablation of Nampt in adult neural stem cells recapitulates their functional defects during aging, EMBO J. 33 (2014) 1321–1340.

[51] X.H. Zhu, M. Lu, B.Y. Lee, K. Ugurbil, W. Chen, In vivo NAD assay reveals the intracellular NAD contents and redox state in healthy human brain and their age dependences, Proc. Natl. Acad. Sci. U. S. A. 112 (2015) 2876–2881.

[52] M. Breton, J.F. Costemale-Lacoste, Z. Li, C. Lafuente-Lafuente, J. Belmin, M. Mericskay, Blood NAD levels are reduced in very old patients hospitalized for heart failure, Exp. Gerontol. 139 (2020), 111051.

[53] S. Lautrup, D.A. Sinclair, M.P. Mattson, E.F. Fang, NAD(+) in brain aging and neurodegenerative disorders, Cell Metabol. 30 (2019) 630–655.

[54] L. Shi, J. Zhang, Y. Wang, Q. Hao, H. Chen, X. Cheng, Sirt1 regulates oxidative stress in oxygen-glucose deprived hippocampal neurons, Front Pediatr 8 (2020) 455.

[55] M. Romashko, J. Schragenheim, N.G. Abraham, J.A. McClung, Epoxyeicosatrienoic acid as therapy for diabetic and ischemic cardiomyopathy, Trends Pharmacol. Sci. 37 (2016) 945–962.

[56] Y. Lee, J.E. Dominy, Y.J. Choi, M. Jurczak, N. Tolliday, J.P. Camporez, H. Chim, J. H. Lim, H.B. Ruan, X. Yang, et al., Cyclin D1-Cdk4 controls glucose metabolism independently of cell cycle progression, Nature 510 (2014) 547–551.

[57] L. Zhao, R. An, Y. Yang, X. Yang, H. Liu, L. Yue, X. Li, Y. Lin, R.J. Reiter, Y. Qu, Melatonin alleviates brain injury in mice subjected to cecal ligation and puncture via attenuating inflammation, apoptosis, and oxidative stress: the role of SIRT1 signaling, J. Pineal Res. 59 (2015) 230–239.

[58] W. Ma, W. Zhang, B. Cui, J. Gao, Q. Liu, M. Yao, H. Ning, L. Xing, Functional delivery of lncRNA TUG1 by endothelial progenitor cells derived extracellular vesicles confers anti-inflammatory macrophage polarization in sepsis via impairing miR-9-5p-targeted SIRT1 inhibition, Cell Death Dis. 12 (2021) 1056.

[59] S. Pushpakumar, L. Ren, S.K. Juin, S. Majumder, R. Kulkarni, U. Sen, Methylation-dependent antioxidant-redox imbalance regulates hypertensive kidney injury in aging, Redox Biol. 37 (2020), 101754.

[60] J. Liu, Z. Zong, W. Zhang, Y. Chen, X. Wang, J. Shen, C. Yang, X. Liu, H. Deng, Nicotinamide mononucleotide alleviates LPS-induced inflammation and oxidative stress via decreasing COX-2 expression in macrophages, Front. Mol. Biosci. 8 (2021), 702107.

[61] K. Chandrasekaran, J. Choi, M.I. Arvas, M. Salimian, S. Singh, S. Xu, R. P. Gullapalli, T. Kristian, J.W. Russell, Nicotinamide mononucleotide administration prevents experimental diabetes-induced cognitive impairment and loss of hippocampal neurons, Int. J. Mol. Sci. (2020) 21.

[62] S. He, Q. Gao, X. Wu, J. Shi, Y. Zhang, J. Yang, X. Li, S. Du, Y. Zhang, J. Yu, NAD(+) ameliorates endotoxin-induced acute kidney injury in a sirtuin1-dependent manner via GSK-3β/Nrf2 signalling pathway, J. Cell Mol. Med. 26 (2022) 1979–1993.

[63] N. Klimova, T. Kristian, Multi-targeted effect of nicotinamide mononucleotide on brain bioenergetic metabolism, Neurochem. Res. 44 (2019) 2280–2287.

[64] S. Tarantini, M.N. Valcarcel-Ares, P. Toth, A. Yabluchanskiy, Z. Tucsek, T. Kiss, P. Hertelendy, M. Kinter, P. Ballabh, Z. Süle, et al., Nicotinamide mononucleotide (NMN) supplementation rescues cerebromicrovascular endothelial function and neurovascular coupling responses and improves cognitive function in aged mice, Redox Biol. 24 (2019), 101192.

[65] A. Das, G.X. Huang, M.S. Bonkowski, A. Longchamp, C. Li, M.B. Schultz, L.J. Kim, B. Osborne, S. Joshi, Y. Lu, et al., Impairment of an endothelial NAD(+)-H(2)S signaling network is a reversible cause of vascular aging, Cell 173 (2018) 74–89. e20.

[66] Y. Zhao, Q. Jiang, X. Zhang, X. Zhu, X. Dong, L. Shen, S. Zhang, L. Niu, L. Chen, M. Zhang, et al., l-Arginine alleviates LPS-induced oxidative stress and apoptosis via activating SIRT1-AKT-nrf2 and SIRT1-FOXO3a signaling pathways in C2C12 myotube cells, Antioxidants (2021) 10.

[67] L. Chen, Z. Wang, Q. Xu, Y. Liu, L. Chen, S. Guo, H. Wang, K. Zeng, J. Liu, S. Zeng, L. Yu, The failure of DAC to induce OCT2 expression and its remission by hemoglobin-based nanocarriers under hypoxia in renal cell carcinoma, Theranostics 10 (2020) 3562–3578.

[68] Y. Xu, L. Liu, B. Pan, J. Zhu, C. Nan, X. Huang, J. Tian, DNA methylation regulates mouse cardiac myofibril gene expression during heart development, J. Biomed. Sci. 22 (2015) 88.

[69] R. Wang, M. Yang, Y. Wu, R. Liu, M. Liu, Q. Li, X. Su, Y. Xin, W. Huo, Q. Deng, et al., SIRT1 modifies DNA methylation linked to synaptic deficits induced by Pb in vitro and in vivo, Int. J. Biol. Macromol. 217 (2022) 219–228.

[70] G. Hu, C. Ling, L. Chi, M.K. Thind, S. Furse, A. Koulman, J.R. Swann, D. Lee, M. M. Calon, C. Bourdon, et al., The role of the tryptophan-NAD + pathway in a mouse model of severe malnutrition induced liver dysfunction, Nat. Commun. 13 (2022) 7576.

[71] B. Xu, P. Zhang, X. Tang, S. Wang, J. Shen, Y. Zheng, C. Gao, P. Mi, C. Zhang, H. Qu, et al., Metabolic rewiring of kynurenine pathway during hepatic ischemia-reperfusion injury exacerbates liver damage by impairing NAD homeostasis, Adv. Sci. 9 (2022), e2204697.
[72] F.J. Oliver, J. Ménissier-de Murcia, C. Nacci, P. Decker, R. Andriantsitohaina, S. Muller, G. de la Rubia, J.C. Stoclet, G. de Murcia, Resistance to endotoxic shock as a consequence of defective NF-kappaB activation in poly (ADP-ribose) polymerase-1 deficient mice, EMBO J. 18 (1999) 4446–4454.
[73] P.O. Hassa, M.O. Hottiger, A role of poly (ADP-ribose) polymerase in NF-kappaB transcriptional activation, Biol. Chem. 380 (1999) 953–959.
[74] Q. Xue, X. Liu, C. Chen, X. Zhang, P. Xie, Y. Liu, S. Zhou, J. Tang, Erlotinib protests against LPS-induced parthanatos through inhibiting macrophage surface TLR4 expression, Cell Death Dis. 7 (2021) 181.
[75] A.R. Fehr, S.A. Singh, C.M. Kerr, S. Mukai, H. Higashi, M. Aikawa, The impact of PARPs and ADP-ribosylation on inflammation and host-pathogen interactions, Genes Dev. 34 (2020) 341–359.
[76] J. Ratajczak, M. Joffraud, S.A. Trammell, R. Ras, N. Canela, M. Boutant, S. S. Kulkarni, M. Rodrigues, P. Redpath, M.E. Migaud, et al., NRK1 controls nicotinamide mononucleotide and nicotinamide riboside metabolism in mammalian cells, Nat. Commun. 7 (2016), 13103.
[77] A. Grozio, K.F. Mills, J. Yoshino, S. Bruzzone, G. Sociali, K. Tokizane, H.C. Lei, R. Cunningham, Y. Sasaki, M.E. Migaud, S.I. Imai, Slc12a8 is a nicotinamide mononucleotide transporter, Nat Metab 1 (2019) 47–57.
[78] J.P. Brás, J. Bravo, J. Freitas, M.A. Barbosa, S.G. Santos, T. Summavielle, M. I. Almeida, TNF-alpha-induced microglia activation requires miR-342: impact on NF-kB signaling and neurotoxicity, Cell Death Dis. 11 (2020) 415.
[79] C. Ren, R.Q. Yao, H. Zhang, Y.W. Feng, Y.M. Yao, Sepsis-associated encephalopathy: a vicious cycle of immunosuppression, J. Neuroinflammation 17 (2020) 14.
[80] T. Manabe, M.T. Heneka, Cerebral dysfunctions caused by sepsis during ageing, Nat. Rev. Immunol. 22 (2022) 444–458.
[81] E. Naik, V.M. Dixit, Mitochondrial reactive oxygen species drive proinflammatory cytokine production, J. Exp. Med. 208 (2011) 417–420.
[82] H. Yang, Z.T. Gu, L. Li, M. Maegele, B.Y. Zhou, F. Li, M. Zhao, K.S. Zhao, SIRT1 plays a neuroprotective role in traumatic brain injury in rats via inhibiting the p38 MAPK pathway, Acta Pharmacol. Sin. 38 (2017) 168–181.
[83] Y. Zhou, J. Li, C. Wang, Z. Pan, Fumitremorgin C alleviates advanced glycation end products (AGE)-induced chondrocyte inflammation and collagen II and aggrecan degradation through sirtuin-1 (SIRT1)/nuclear factor (NF)-κB/mitogen-activated protein kinase (MAPK), Bioengineered 13 (2022) 3867–3876.
[84] B. Li, C. Dasgupta, L. Huang, X. Meng, L. Zhang, MiRNA-210 induces microglial activation and regulates microglia-mediated neuroinflammation in neonatal hypoxic-ischemic encephalopathy, Cell. Mol. Immunol. 17 (2020) 976–991.
[85] Q. Li, J.X. Tan, Y. He, F. Bai, S.W. Li, Y.W. Hou, L.S. Ji, Y.T. Gao, X. Zhang, Z. H. Zhou, et al., Atractylenolide III ameliorates non-alcoholic fatty liver disease by activating hepatic adiponectin receptor 1-mediated AMPK pathway, Int. J. Biol. Sci. 18 (2022) 1594–1611.
[86] J. Zhang, R. Bi, Q. Meng, C. Wang, X. Huo, Z. Liu, C. Wang, P. Sun, H. Sun, X. Ma, et al., Catalpol alleviates adriamycin-induced nephropathy by activating the SIRT1 signalling pathway in vivo and in vitro, Br. J. Pharmacol. 176 (2019) 4558–4573.
[87] M.J. Delano, P.A. Ward, The immune system's role in sepsis progression, resolution, and long-term outcome, Immunol. Rev. 274 (2016) 330–353.
[88] F. Pei, R.Q. Yao, C. Ren, S. Bahrami, T.R. Billiar, I.H. Chaudry, D.C. Chen, X. L. Chen, N. Cui, X.M. Fang, et al., Expert consensus on the monitoring and treatment of sepsis-induced immunosuppression, Mil Med Res 9 (2022) 74.
[89] V.T. Vachharajani, T. Liu, C.M. Brown, X. Wang, N.L. Buechler, J.D. Wells, B. K. Yoza, C.E. McCall, SIRT1 inhibition during the hypoinflammatory phenotype of sepsis enhances immunity and improves outcome, J. Leukoc. Biol. 96 (2014) 785–796.